Dewey G. McCafferty
Predrag Cudic
Brenda A. Frankel
Salim Barkallah
Ryan G. Kruger
Wenkai Li
Department of Biochemistry and Biophysics and the Johnson Research Foundation, The University of Pennsylvania School of Medicine, Philadelphia, PA 19104-6059

Chemistry and Biology of the Ramoplanin Family of Peptide Antibiotics

Abstract: *The peptide antibiotic ramoplanin factor A2 is a promising clinical candidate for treatment of Gram-positive bacterial infections that are resistant to antibiotics such as glycopeptides, macrolides, and penicillins. Since its discovery in 1984, no clinical or laboratory-generated resistance to this antibiotic has been reported. The mechanism of action of ramoplanin involves sequestration of peptidoglycan biosynthesis Lipid intermediates, thus physically occluding these substrates from proper utilization by the late-stage peptidoglycan biosynthesis enzymes MurG and the transglycosylases (TGases). Ramoplanin is structurally related to two cell wall active lipodepsipeptide antibiotics, janiemycin, and enduracidin, and is functionally related to members of the lantibiotic class of antimicrobial peptides (mersacidin, actagardine, nisin, and epidermin) and glycopeptide antibiotics (vancomycin and teicoplanin). Peptidomimetic chemotherapeutics derived from the ramoplanin sequence may find future use as antibiotics against vancomycin-resistant* Enterococcus faecium *(VRE), methicillin-resistant* Staphylococcus aureus *(MRSA), and related pathogens. Here we review the chemistry and biology of the ramoplanins including its discovery, structure elucidation, biosynthesis, antimicrobial activity, mechanism of action, and total synthesis.* © 2002 Wiley Periodicals, Inc. Biopolymers (Pept Sci) 66: 261–284, 2002

Keywords: *ramoplanin; peptide antibiotics; bacterial infections; peptidoglycan biosynthesis; Lipid; lipodepsipeptide; antimicrobial peptides; peptidomimetic chemotherapeutics; pathogens*

INTRODUCTION

For many decades antimicrobial chemotherapy has been utilized successfully for the treatment of infectious disease. However, the widespread use of broad-spectrum antibiotics has placed enormous selective pressures on bacterial populations, forcing the evolution of resistance mechanisms. Initially, as resistance

Correspondence to: Dewey G. McCafferty, Department of Biochemistry and Biophysics, The University of Pennsylvania School of Medicine, 905A Stellar-Chance Building, 422 Curie Blvd., Philadelphia, PA 19104-6059; email: deweym@mail.med.upenn.edu

Contract grant sponsor: National Institutes of Health (NIH), American Cancer Society (ACS), and McCabe Foundation; contract grant number: AI46611 (NIH) and RPG-99-31-02-CCE (ACS)

Biopolymers (Peptide Science), Vol. 66, 261–284 (2002)

© 2002 Wiley Periodicals, Inc.

arose against one class of antibiotics, such as the penicillins, the problem was overcome by the introduction of new classes of antibiotics, such as the aminoglycosides, macrolides, and glycopeptides, as well as the chemical modification of existing drugs. Unfortunately, over the past decade, antibiotic resistance has emerged in virtually all hospital-acquired pathogen–antimicrobial agent combinations.

Since about 5% of all patients admitted to acute-care hospitals acquire opportunistic infections, inhibiting bacterial colonization is of paramount importance clinically. Seven leading pathogen groups have accounted for most of the increase in hospital-acquired (nosocomial) infections in the United States between 1980 and present: *Escherichia coli,* coagulase-negative *Staphylococci, Streptococcus, Pseudomonas aeruginosa, Staphylococcus aureus, Enterococcus faecium,* and *Candida albicans*—the majority of which are Gram-positive bacteria. Patients recovering from invasive surgery or burn trauma, or with long-term intravenous lines, intercranial shunts, and indwelling catheters are at high risk for developing opportunistic infections from these organisms. Likewise, individuals immunocompromised due to organ transplantation, HIV-AIDS, or intensive chemotherapy of leukemia, lymphoma, or other neoplastic cancers are vulnerable to nosocomial infection. Antibiotic resistance results in morbidity and mortality from treatment failures and increased health care costs, presently estimated by the National Centers for Disease Control and Prevention to be over $4 billion annually. Given our dwindling arsenal of effective antibiotics, primarily consisting of vancomycin, the drug of last resort for treatment of Gram-positive pathogens, it is not difficult to see a time when our most serious infectious threats will be untreatable.

The peptide antibiotic ramoplanin factor A2 (**2,** Figure 1) is emerging as a promising clinical candidate for treatment of Gram-positive bacterial infections, particularly those that are resistant to antibiotics such as glycopeptides, macrolides, and penicillins. Remarkably, since its discovery in 1984, no clinical or laboratory-generated resistance to this antibiotic has been reported. The mechanism of action of ramoplanin is unique in that it involves sequestration of peptidoglycan biosynthesis Lipid intermediates, thus physically occluding these substrates from proper utilization by the late-stage peptidoglycan biosynthesis enzymes MurG and the transglycosylases (TGases) (Figure 2). Recent studies on the molecular mechanism of action of ramoplanin, combined with a newly reported total synthesis, now make possible the rational examination of structure-activity relationships, the evaluation of a bioactive pharmacophore, and the generation of ramoplanin sequence-derived peptidomimetics. Here we review the chemistry and biology of this important new class of peptide antibiotics, focusing on the discovery, structure elucidation, biosynthesis, antimicrobial activity, mechanism of action, and total synthesis of the lipodepsipeptide antibiotic ramoplanin. Structural and functional relationships of the ramoplanin family of peptide antibiotics to the enduracidin, lantibiotic, and glycopeptide antibiotic families are also reviewed.

RAMOPLANINS A1-A3 AND RAMOPLANOSE: DISCOVERY AND STRUCTURE ELUCIDATION

Discovery

Ramoplanin factors A1 (**1**), A2 (**2**), and A3 (**4**) were discovered in 1984 in the course of a Biosearch Italia (formerly Gruppo Lepetit SPA, Italy) industrial drug discovery program aimed at identifying novel antibiotics active against bacterial cell wall production from the culture broth of actinomycetes (members of the genus *Actinoplanes*) (Figure 1).[1,2] This discovery program relied on the development of a specific culture media that allowed the researchers to isolate in pure culture numerous *Actinoplanes* strains. Cell wall active antibiotics were identified from the actinomycetes culture broth based on the selective killing of methicillin-resistant *Staphylococcus aureus* over the L-form of *S. aureus* (a form lacking cell wall synthesis when cultured in hypotonic medium). Thus ramoplanin factors A1, A2, and A3 were isolated in 12, 72, and 16% yields, respectively, from purification of the culture broth of *Actinoplanes* strain ATCC 33076. Ramoplanins A1–3 differ in the length of the *N*-terminal acyl chain, but all have nearly identical antimicrobial activity (Figure 1). Soon after the discovery and isolation of factors A1–3, the media formulation was changed and the host producing strain was genetically manipulated to increase the content of factor A2 and decrease the combined content of factors A1 and A3 to $\leq$15% of the total ramoplanins.[2]

Three additional ramoplanin factors designated A′1, A′2, and A′3 were later shown to be present in the fermentation medium, and were shown to differ from the A1, A2, and A3 components of the original complex by lacking one mannose unit from the glycosidic group.[3] Bioconversion of A factors into A′ factors was achieved by incubation with the mycelium of Actinoplanes ATCC 33076. Factor A′2 has better antibacterial activity than A2 against some bacteria.[3]

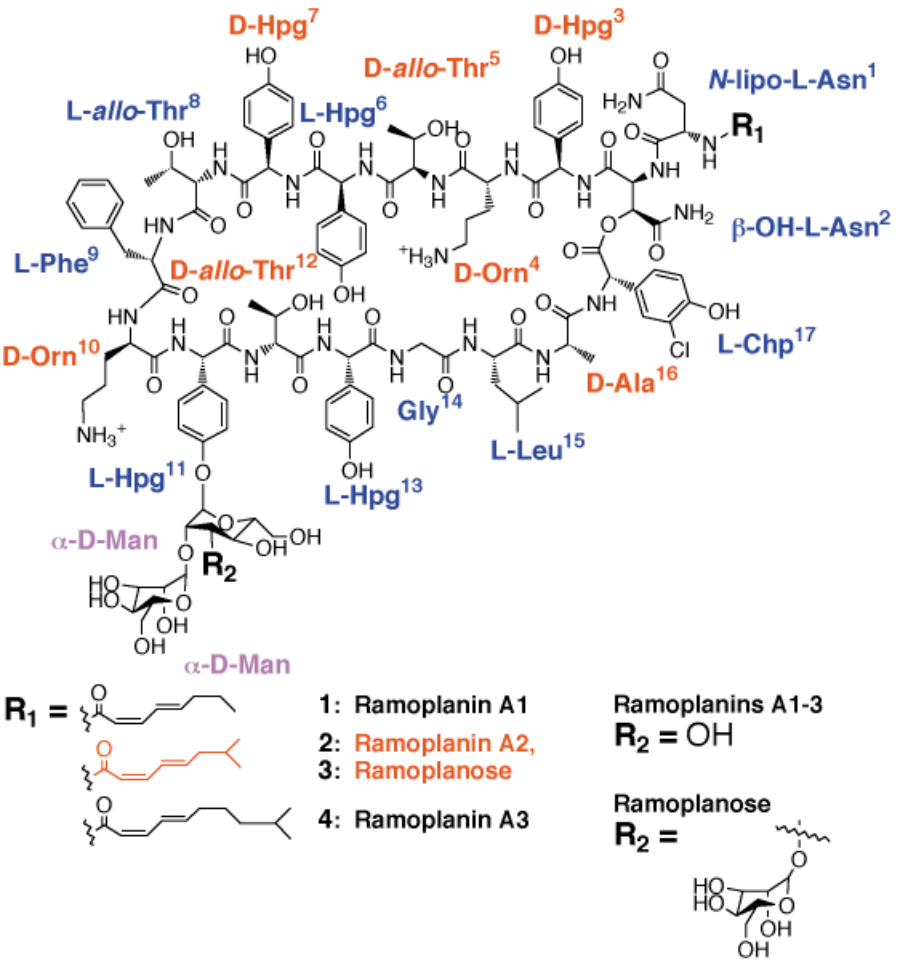

FIGURE 1 Chemical structures of members of the ramoplanin family of lipoglycodepsipeptide antibiotics. D-Amino acids are depicted in red letters, L-amino acids in blue letters, and the pendant mannosyl carbohydrate in magenta. Ramoplanins A1–A3 contain the same peptide core and carbohydrate modification, but they differ in the composition of the *N*-terminal acyl chain. Ramoplanin A2 and ramoplanose only differ by the presence of an additional D-mannose sugar.

Soon after the discovery of ramoplanins A1–3, Pfizer Central Research discovered the related antibiotic ramoplanose (**3,** also known as UK-71,903) from fermentation of an unnamed *Actinoplanes* species (Figure 1). Structural differences and similarities between ramoplanins A1–A3 and ramoplanose are described below. Unfortunately, no information about the biological activity of ramoplanose has been reported since its discovery.

Structure Elucidation

Using a combination of chemical degradation, ^{1}H and ^{13}C NMR, and mass spectrometery studies, the structures of the three components of the antibiotic ramoplanin (formerly A/16686) were elucidated by Ciabatti and co-workers.[4] In a companion paper, Kettering and colleagues confirmed the sequence of ramoplanin A2 using multidimensional NMR techniques.[5] All the components have structures formed by a common depsipeptide skeleton carrying a dimannosyl group, and are differentiated by the presence of various acylamide moieties, derived from C_8, C_9, and C_{10} fatty acids (Figure 1). Ramoplanins contain an abundance of hydroxyphenylglycines (Hpg) of both D and L configurations as well as numerous β-hydroxylated amino acids (D,L *allo*-Thr; *threo*-β-OH–Asn). The *N*- and *C*-termini of ramoplanin are covalently linked by a lactone bridge between the 3-chloro-4-hydroxyphenylglycine residue (Chp^{17}) and the side-chain hydroxyl of β-hydroxyasparagine (β-OH–Asn^2), forming a 49-membered ring.

Soon after the structure of ramoplanin A2 was described, Williams and co-workers determined the

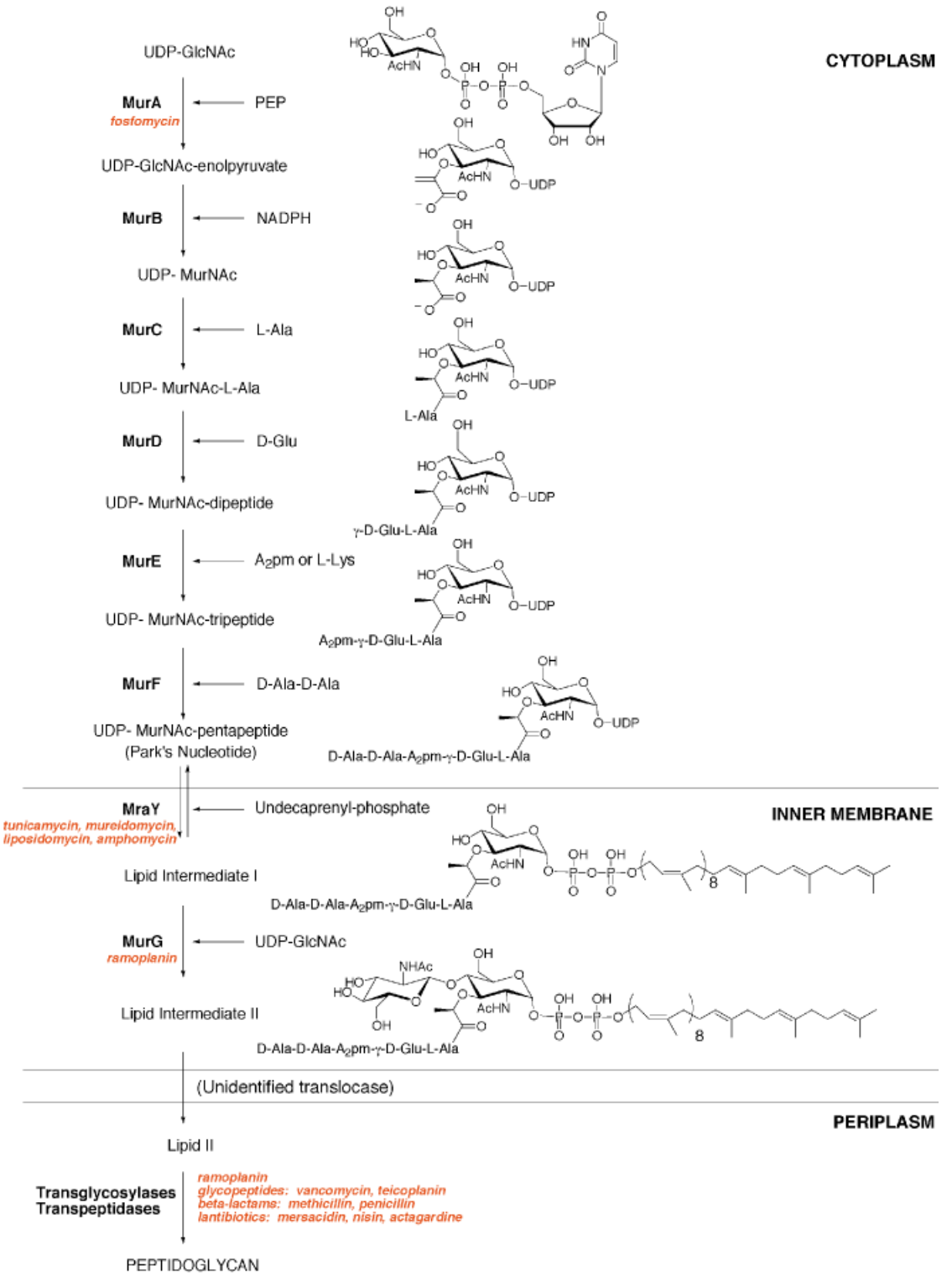

FIGURE 2 Biosynthesis of bacterial peptidoglycan. Antibiotics interrupting this pathway are highlighted in red. Ramoplanin A2 interrupts the late-stage glycosyltransferase activities of MurG and the transglycosylase (TGase).

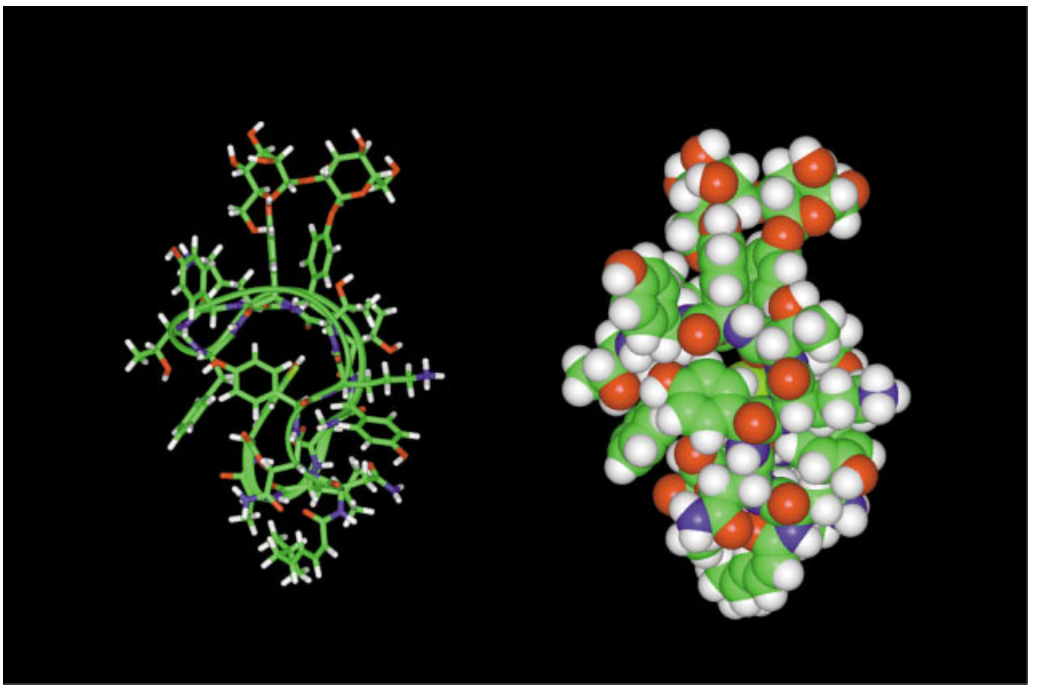

FIGURE 3 Stick and space-filling (CPK) representations of the three-dimensional structure of ramoplanin A2 as determined by Kurz and Guba. Coordinates for the ramoplanin A2 NMR structure have been deposited in the Protein Databank under the accession number 1DSR.

composition and three-dimensional solution structure of the related antibiotic ramoplanose using NMR methods in conjunction with chemical degradation and mass spectrometry studies.[6] Williams found ramoplanose to be identical in composition to ramoplanin A2 with the exception of the branched mannose trisaccharide attached to Hpg^{11} (ramoplanin A2 contains an $\alpha(1\rightarrow2)$-linked D-mannosyl disaccharide). Ramoplanose was described as possessing an antiparallel two-stranded β-sheet defined by seven intramolecular hydrogen bonds and two reverse turns. One peptide strand contains a β-bulge. As the peptide strands extend away from the Thr^8–Phe^9 reverse turn, their chiralities alternate in pairs (D/D then L/L). In the context of a β-sheet, this arrangement of residue chiralities forces the amino acid side chains to adopt adjacent positions on one side of the antiparallel β-sheet. To relieve steric strains due to this juxtaposition, the peptide backbone curves significantly, giving the antibiotic a cup-like architecture. The regiochemistry of the 7-methyloctadi-2,4-enoic acid *N*-acyl group was established unequivocally as *cis*–transoid–*trans*.

In 1996, Kurz and Guba determined the three-dimensional structure of the clinically important ramoplanin A2 in 20% DMSO using multidimensional NMR methods.[7] Space-filling and stick representations of the structure of ramoplanin A2 are depicted in Figure 3. Kurz and Guba confirmed the similarity in overall architecture of ramoplanin A2 to ramoplanose, and they also revised the regiochemistry of the double bonds of the 7-methyloctadi-2,4-enoic acid group to *cis–trans* since previously it had been assigned as *cis–cis*.[4] Several factors help define the conformation of ramoplanin A2, including the presence of six hydrogen bonds bridging the two antiparallel β-strands, a buried core of orthogonally packed hydrophobic residues (Phe^7, Hpg^3, and Chp^{17}), the conformationally constraining intramolecular macrocyclic lactone bond, and steric constraints imposed by the pendant disaccharide (Figure 1).

To date, no x-ray crystal structure has been reported for any member of the ramoplanin family. However, in preparation for crystallographic analyses of ramoplanin A2 and its complex with peptidoglycan-derived ligands, McCafferty and Loll have obtained crystals of ramoplanin A2 and heavy atom derivatives that diffract to 2.1 Å (Figure 4, P. J. Loll and D. G. McCafferty, unpublished results). At the time of submission of this review, full data sets have been obtained and our laboratories are working to solve the crystal structure.

FIGURE 4 The 2.1 Å diffracting crystals of ramoplanin A2.

BIOSYNTHESIS OF RAMOPLANIN

Nonribosomal Peptide Synthesis

Many low-molecular-weight peptides of microbial origin are synthesized nonribosomally on large multifunctional proteins, termed nonribosomal peptide synthetases (NRPSs). Common to these synthetases are repeated modular defined domains that catalyze specific reactions of peptide synthesis. The order of these domains within the enzyme determines the sequence and structure of the peptide product. For each amino acid in the peptide sequence, NRPS enzymes contain unique tri-functional modules comprised of condensation (C), adenylation (A), and thiolation (T) domains. NRPS active sites of C, A, and T domains are highly organized so that a specific amino acid is recognized and incorporated into the peptide sequence. Detailed sequence, mutational, and structural analyses of A-domain active sites of NRPS synthetases by the Marahiel[8] and Townsend groups[9] have revealed a unique NRPS specificity code that has been successfully employed as a predictor of the amino acid sequence of the peptide product.[10]

Within a tri-functional C-A-T module, the A domain activates the amino acid as an adenylate for subsequent attachment to the T domain (also called a peptidyl carrier protein or PCP). The resultant aminoacyl adenylate is attached to the NRPS T domain by thiol attack from an enzyme-bound phosphopantetheine cofactor, which forms an enzyme–acyl thioester linkage. Peptide bond formation is then catalyzed by the C domain, which joins the pendant T domain amino acid with an activated aminoacyl intermediate bound to the T domain of an adjacent C-A-T module. This results in a dipeptide fixed to the T domain of the second module and the regeneration of the T domain in the preceding module. This process continues in a stepwise "assembly line" fashion until the full-length peptide is assembled, after which the peptide is released by the action of a *C*-terminal thioesterase domain (TE domain) that hydrolyzes the thioester, and in specific cases, is also responsible for peptide macrocyclization.

Additional important tailoring enzymes are found within antibiotic biosynthetic loci. The primary sequence of NRPS-produced peptide antibiotics may be further modified by halogenation, epimerization, hydroxylation, methylation, glycosylation, etc. These modifications may occur prior to, during, or immediately after NRPS peptide assembly. Tailoring enzymes are found both as part of the NRPS, such as a methylation or epimerization internal domain, or as external neighboring genes contained within the biosynthetic locus. Genes encoding pathways for the biosynthesis of amino acid, polyketide, or fatty acid precursors, and those responsible for antibiotic export or for producer immunity, are often located near the NRPS in the biosynthetic locus. Harnessing the potential of the gene products within antibiotic biosynthetic loci has widespread potential applications in bioengineering, particularly in applications directed toward improving antibiotic production, improving chemical/biological properties, and generating new bioactive molecules.

The Ramoplanin Biosynthetic Gene Locus

Farnet and co-workers recently cloned and sequenced the 88.5 kilobase (kb) ramoplanin biosynthetic gene locus from *Actinoplanes* ATCC 33076.[11] As shown in Figure 5, the ramoplanin biosynthetic gene locus contains 33 genes responsible for a myriad of functions including amino acid (Orfs 4, 6, 7, 28, 30), fatty acid (Orfs 9, 16, 24, 25, 26, 27) and peptide biosynthesis (Orfs 11, 12, 13, 14, 15, 17), polypeptide tailoring (Orfs 10, 20), antibiotic export/producer resistance (Orfs 2, 8, 23, 31), and transcriptional regulation (Orfs 5, 21, 22, 33). A summary of the putative gene functions and related genes identified by homology searches appears in Table I.

Ramoplanin NRPS Architecture

The ramoplanin peptide core is assembled by the combined action of four NRPS genes, Orfs 12, 13, 14, and 17. Sequence analysis of these genes revealed condensation, adenylation, and thiolation domains for 16 out of the 17 amino acids (Figure 6). Examination of the adenylation domains predict that Orf 12 contains a C-A-T module for Asn, so it appears that Orf 12 is used twice, once for Asn^1 and again for β-OH Asn^2. Orf 13 is considerably larger, containing C-A-T modules for residues Hpg^3–Phe^9, with the exception of a missing adenylation domain for Thr^8. However, Orf 17 probably provides this missing adenylation domain since it contains an isolated Thr-encoded A-T

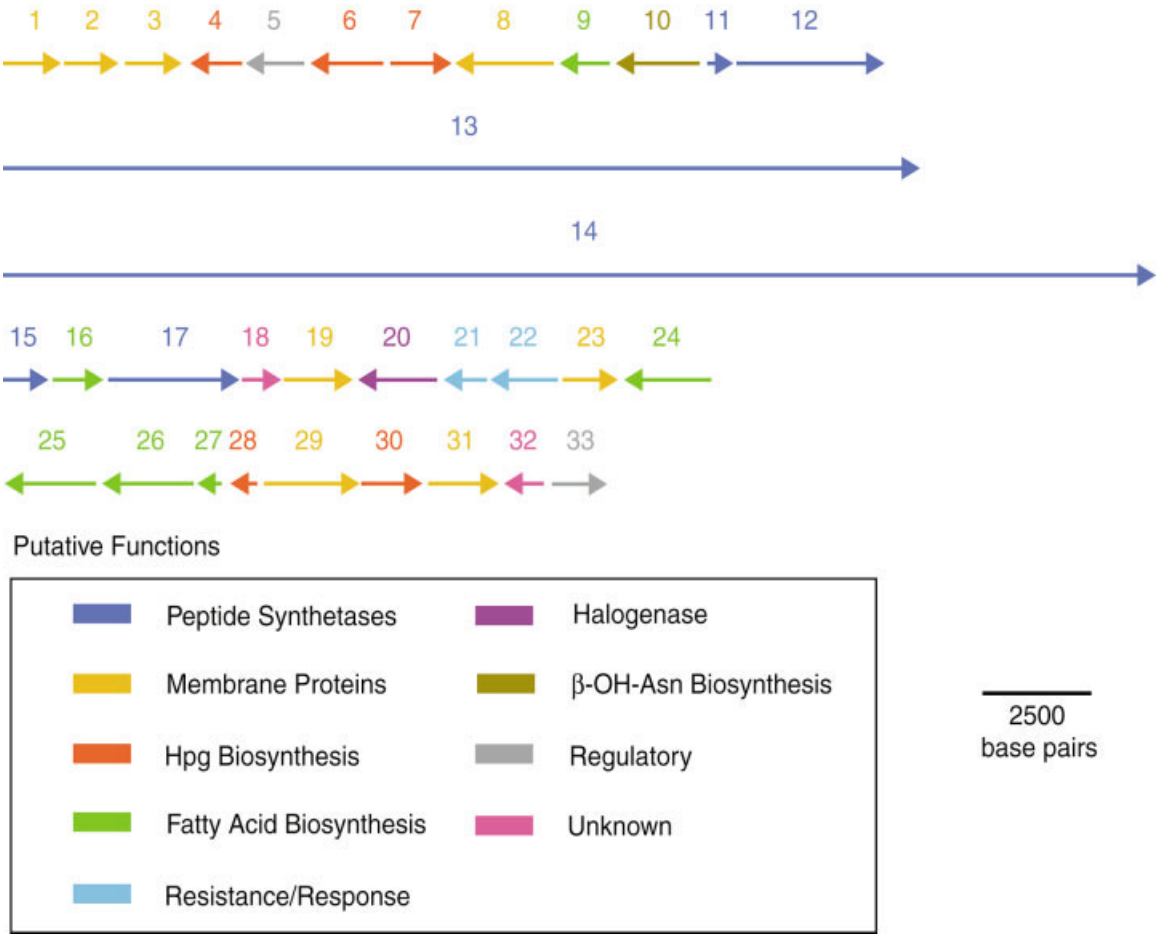

FIGURE 5 Arrangement of open reading frames in the ramoplanin A2 biosynthetic gene locus.

domain. Thus Thr^{8} is unusual in that it is activated by Orf 17 then condensed with Orf 13 in *trans*. Orf 14 continues the assembly of the peptide chain, with C-A-T modules coding for D-Orn^{10}–Chp^{17}. Interestingly, although ramoplanin contains an abundance of D-amino acids, there are no epimerization domains contained within the NRPS Orfs. Located at the *C*-terminus of Orf 14 is a small thioesterase domain that cleaves the ramoplanin peptide thioester from the carrier thiolation domain with concomitant Asn^{2}–Chp^{17} macrolactonization.

Biosynthesis of Ramoplanin Precursors

Orfs 4, 6, 7, and 30 closely resemble the Hpg biosynthetic machinery in the biosynthetic gene clusters of chloroeremomycin and complestatin.[12–14] Like these natural products, Hpg is formed from prephenate through the predicted prephenate dehydrogenase, hydroxyphenylglycine transaminase (HpgT), hydroxymandelate oxidase (Hmo), and hydroxymandelate synthase (HmaS) activities of these proteins (Figure 7). However, the ramoplanin gene cluster also contains a fifth enzyme, Orf 28, which shows high sequence similarity to chorismate mutase (Table I). Therefore, an additional step may be present in the ramoplanin Hpg biosynthetic pathway as compared to that of chloroeremomycin and complestatin. The presence of Orf 28 would suggest that chorismate is an abundant precursor for Hpg in *Actinoplanes* ATCC 33076; thus either chorismate, prephenate, or tyrosine may be employed as starting substrates.

At present, the stereochemical outcome of the Hpg pathway is unknown. No epimerization domains are located in NRPS Orfs 13 and 14. However, since D- and L-Hpg residues are found in ramoplanin, either the enzymes of the Hpg biosynthetic pathway or the adenylation domains are D/L-enantioselective or intracellular epimerases assist in production of the alternate stereoisomer.

Ramoplanin's acyl chain is likely produced from the C_7 precursor depicted in Figure 8. The presence of candidate acyl carrier proteins (ACPs) (Orfs 11, 27) and an acyl–CoA ligase (Orf 26) would suggest that

Table I Summary of Genes Identified in the Ramoplanin Biosynthetic Gene Cluster

ORF (Name)	Position in Base Pairs (Start–Stop)	Size (Amino Acids)	Proposed Function	Accession Numbers of Homologous Proteins
1	2077–3078	333	Unknown membrane protein	CAB48902
2	3118–4032	204	ABC transporter	CAB48901, AAF12291
3	4038–5048	321	Unknown membrane protein	CAB48902
4*	6665–5814	283	Prephenate dehydrogenase	CAA11792, CAB38592
5*	7703–6693	336	Regulatory protein	CAA07385, CAB45047
6	9464–8130	444	Aminotransferase	CAB38598, CAA11790
7	9691–10761	356	Hydroxymandelate oxidase	CAB38520, AAA34030
8*	12751–10829	640	Glycopeptide ABC transporter	CAA11793, AAF67494
9*	13617–12802	271	Type II thioesterase	CAB38877, CAA11784
10*	15203–13614	529	Hydroxylase	AAB30311
11	15591–15863	90	PCP/ACP	AAA22001, AAF62883
12 (RAMO A)	15880–19035	1051	Peptide synthetase	CAB15186, AAD56240
13 (RAMO B)	19032–39713	6893	Peptide synthetase	AAC80285, AAC45930
14 (RAMO C)	39713–65800	8695	Peptide synthetase	AAC80285, AAC45930
15	65826–66530	234	Type II thioesterase	AAC69333, AAC01736
16	66546–67370	274	NAD dependent ACP reductase	AAC44307, CAA77599
17	67384–70059	891	Peptide synthetase	CAA67248, AAC38442
18	70099–70662	187	Unknown	None
19	70659–71906	415	Transmembrane protein	CAB42730, CAB02537
20*	73439–71964	491	Halogenase	CAA11780, CAA76550
21*	74216–73563	217	Resistance/response	CAB59507, CAB38597
22*	75424–74213	403	Resistance/response	CAB42041, CAB38596
23	75535–76464	309	ABC transporter	CAB48901, AAF12291
24*	78110–76449	553	FAD dependent Acyl-CoA dehydrogenase	AAD45605, CAB55554
25*	79864–78107	585	FAD dependent Acyl-CoA dehydrogenase	CAB61531, CAB07077
26*	81624–79861	587	Acyl CoA ligase	AAG02359, AAB52538
27*	81909–81682	75	ACP/PCP	CAB38589, CAB08480
28*	82346–82062	94	Chorismate mutase	CAB02002, CAB72783
29	82587–84446	619	Transmembrane protein	CAB16086, CAA05568
30	84481–85548	355	Hydroxymandelate synthase	CAA11761, AAA50231
31	85556–86845	429	Na/H antiporter	CAB45049, BAA16991
32*	87372–86803	189	Unknown	CAB72201, CAB56690
33	87494–88420	309	Regulatory	CAB95285, CAC44680

* Gene on opposite strand.

either an acyl–CoA or an acyl–ACP is the true acyl precursor substrate. In analogy to fatty acid biosynthesis, Orfs 24 and 25 are putative FAD-dependent dehydrogenases and Orf 16 is a putative NAD-dependent reductase with similarity to 3-oxoacyl ACP reductases (Table I). These enzymes likely work together to generate the unique *cis-trans* double bond regiochemistry found in the *N*-acyl chain. Intriguingly, no ketosynthase is present in the biosynthetic gene cluster, but this activity may be borrowed from primary metabolism. The mature fatty acid is probably transferred via an ACP (possibly Orf 11 or 27) to Orf 12-bound Asn^1 to form the starter unit. It is important to note that putative ACP/PCPs (Orfs 11, 27) and type II thioesterases (Orfs 9, 15) are also found within the biosynthetic locus. Assembly of the acyl chain could involve the contribution of one or all of these gene products.

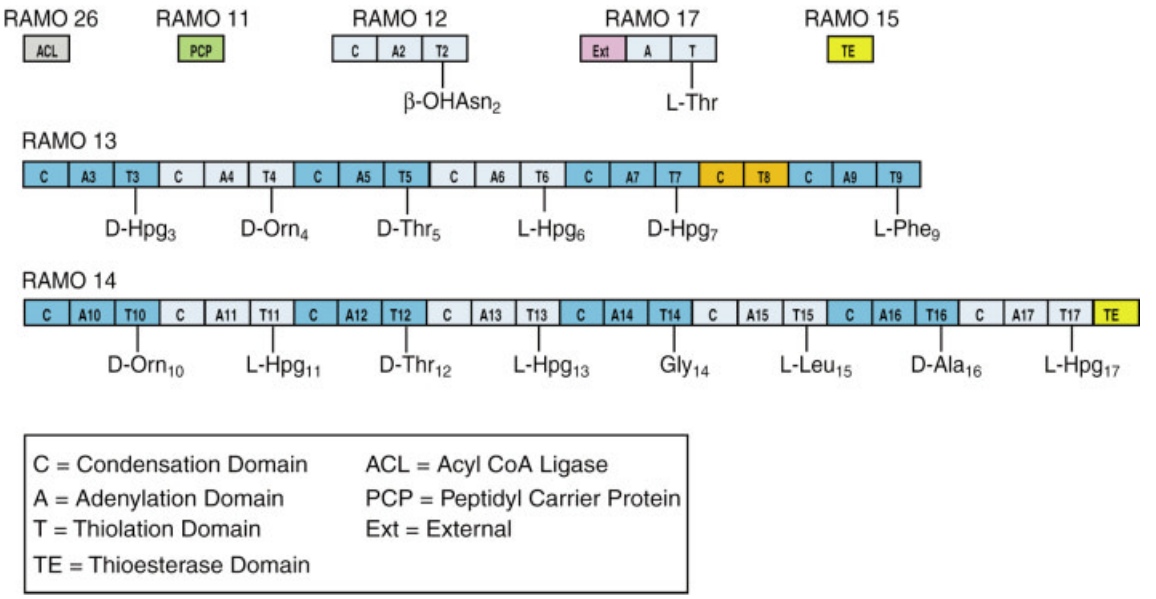

FIGURE 6 Organization of the nonribosomal peptide synthetases found in the ramoplanin A2 biosynthetic gene locus. Orf 12 contains activation, thiolation, and condensation domains for assembly of the starter unit of Asn^1 and Asn^2 residues. The latter residue is subsequently β-hydroxylated. Residues 3–9 are assembled using two NRPS enzymes, Orf 13 and Orf 17. Orf 13 contains condensation, activation, and thiolation domains associated with assembly of residues 3–7 and 9, but only contains condensation and thiolation domains for Thr^8. The missing adenylation domain and a thiolation domains for Thr^8 are found separately on a small NRPS (Orf 17). Thr^8 assembly therefore requires the coordinate interaction of Orf 13 and Orf 17 for peptide bond formation. Lastly, Orf 14 is an NRPS that codes for the assembly of the remaining residues 10–17. Orf 14 terminates with a thioesterase (TE) domain that is responsible for cleavage and concomitant peptide cyclization. There are no epimerization domains present in any of the NRPS open reading frames.

Tailoring Enzymes

Ramoplanin contains three covalent amino acid modifications. Asn^2 is β-hydroxylated, Hpg^{11} is glycosylated, and Hpg^{17} is chlorinated. However, the biosynthetic locus offers clues to only two of these modifications. No glycosyl transferases were identified in the locus, and although ramoplanin could be a substrate for cellular glycosyl transferases, such a relationship has not yet been demonstrated. Orf 10, predicted to be a non-heme Fe-hydroxylase, is the candidate enzyme for β-hydroxylation of Asn^2. Orf 20 shows high homology to known halogenases involved in the chlorination of secondary metabolites and is the probable halogenase involved in production of Chp^{17}.

Regulation, Export, and Immunity

In addition to the enzymes responsible for assembly and covalent modification of ramoplanin, there are a number of ORFs bearing similarity to proteins and enzymes involved in transcriptional regulation or immunity (Orfs 5, 21, 22, 33) and transport (Orfs 2, 8, 23, 31). Orfs 1, 3, 18, 19, 29, and 32 are proteins of unknown function for which little homology to known proteins exists. However, some of these proteins contain predicted transmembrane domains that might suggest their involvement in transport, transcriptional regulation, or immunity.

ANTIMICROBIAL ACTIVITY

Antimicrobial Activity and Specificity Studies

Ramoplanin exhibits broad-spectrum and potent *in vitro* and *in vivo* activity against Gram-positive bacteria. Espensen's 1999 review on the clinical progress of ramoplanin neatly outlined results from antimicrobial specificity testing.[15] We will therefore briefly summarize these results. Ramoplanin is active against a wide variety of Gram-positive bacteria[16,17] including enterococci,[18–24] staphylococci,[17,18,24–32] bacilli,[20]

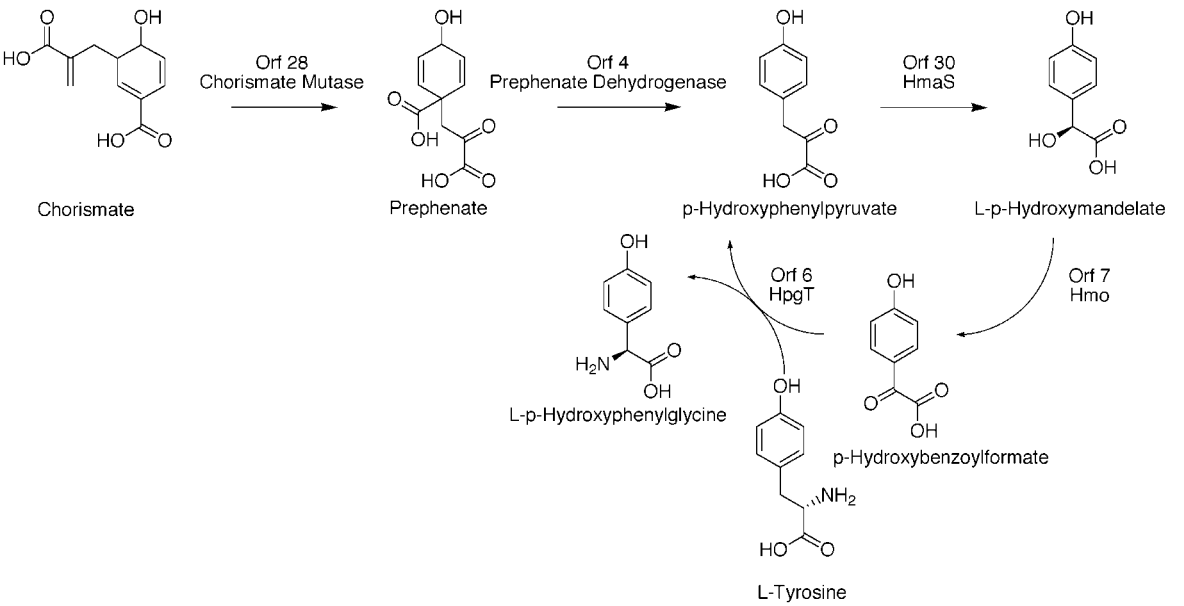

FIGURE 7 Pathway for biosynthesis of 4-hydroxyphenylglycine from the ramoplanin A2 gene locus.

streptococci,[24,27,33,34] *Listeria monocytogenes,*[20] and Gram-positive anaerobes such as *Clostridium difficile.*[23,31,33,35–37]

Ramoplanin susceptible *S. aureus* strains and MRSA have low MIC values ($\leq$2.0 μg/mL). Coagulase-negative staphylococci have MIC values up to 8 μg/mL.[38] Streptococci, pneumococci (including penicillin-resistant strains), *Corynebacterium sp.*, and *Propionibacterium acnes* are susceptible with MIC values of $\leq$2 μg/mL.[37] VRE is also potently inhibited by ramoplanin with a MIC of $<$1 μg/mL, and it experiences a bacteriocidal effect at twice the MIC value.[39] The antibiotic also has bacteriocidal activity against MRSA and enterococci.[37,40] Ramoplanin MIC values are not inhibited by an inoculum of up to 10^7 colony-forming units, but the bacteriocidal activity can be modulated by the addition of serum or serum albumin.[41] Ramoplanin has no activity against Gram-negative bacteria.[16,30] Furthermore, no clinical or laboratory-generated resistance to ramoplanin has been reported.

Clinical Results and Applications

In multiple Phase I clinical trials, ramoplanin proved to be safe and well tolerated at all tested doses. Ramoplanin treatment of patients with symptomatic pseudomembraneous colitis (PMC) was examined in Phase I trials using six male subjects given a single oral dose of 200 mg. No detectable concentrations of ramoplanin were found in serum or urine.[42] Maximum concentration in stool was 392 μg/g. No adverse effects were reported. Repeated oral divided doses in healthy human volunteers demonstrated a lack of absorption (no detectable levels in urine or plasma), and a lack of deleterious effect on fecal flora.[43] However, suitable concentrations were available for treatment of Gram-positive pathogens. An animal model of gastrointestinal colonization with VRE showed significant suppression of bacterial growth, although colonization recurred after ramoplanin administration was discontinued.[44]

Ramoplanin was licensed to IntraBiotics for Phase II efficacy trials for elimination of intestinal VRE. Bloodstream infections due to VRE pose a particular risk in patients with compromised immune systems. At-risk populations include patients undergoing chemotherapy, organ transplantation, or any kind of immunosuppressive regimen, and patients in the intensive care unit. By eliminating the reservoir of VRE in the gut, physicians believe that the incidence of VRE bloodstream infections may be reduced. Phase II trial results demonstrated that ramoplanin significantly reduced VRE gastrointestinal colonization in hospitalized patients. Wong and co-workers evaluated the safety and efficacy of oral ramoplanin versus a placebo for suppression of gastrointestinal VRE colonization.[45] Results showed that ramoplanin eradicated gastrointestinal VRE in 90% of the patients undergoing treatment; by comparison, all placebo patients had detectable VRE. The Phase II protocol was originally

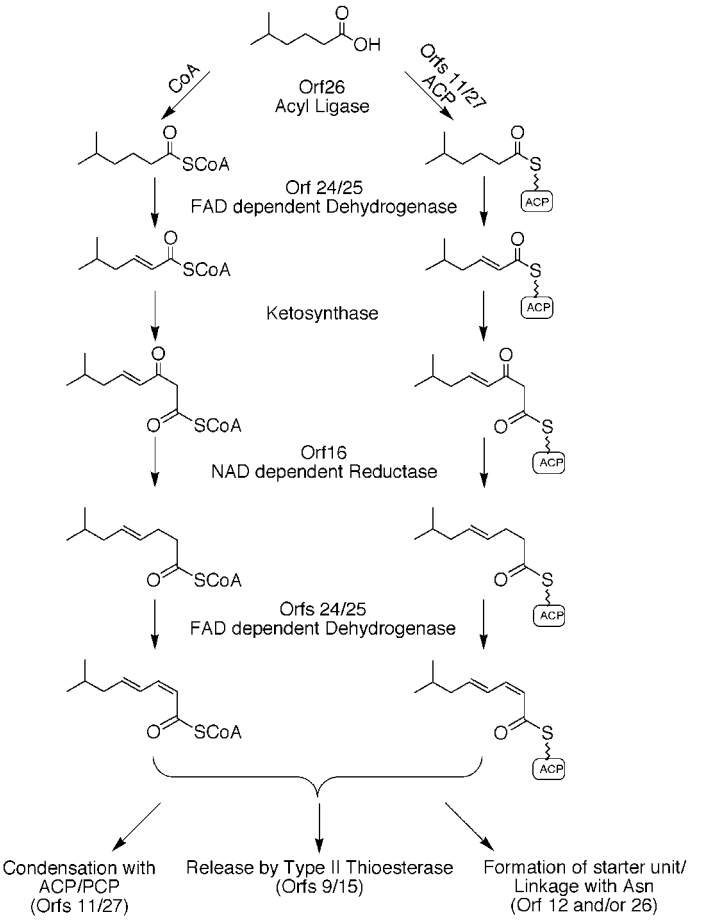

FIGURE 8 Biosynthesis of the *N*-terminal methyl-octadi-2,4-enoic acid.

designed for a total of 150 patients; however, enrollment was terminated early (after 68 patients were treated) at the recommendation of an independent Data and Safety Monitoring Board (DSMB). The DSMB determined that ramoplanin had already shown sufficient evidence of effectiveness and safety, and suggested that the product proceed to Phase III trials. In a related study, Moellering and co-workers recently reported the molecular characterization of VRE that was found to repopulate the gastrointestinal tract following treatment with ramoplanin.[46]

In October 2001, the rights to develop and market ramoplanin as an agent for the prevention of bloodstream infections caused by VRE in the United States were transferred from Biosearch Italia to Genome Therapeutics Corp. A 950-patient, Phase III clinical trial is currently underway at more than 40 sites in the United States. In response to the pressing threat of rising antimicrobial resistance and VRE infections, the U.S. Food and Drug Administration (FDA) has designated Fast Track status for ramoplanin, reflecting its potential to address an unmet medical need for a serious, life-threatening condition.

The lack of systemic absorption of ramoplanin has limited clinical applications of oral formulations of the drug to the treatment of gastrointestinal carriage, nasal staphycoccal carriage,[15] and antibiotic-associated diarrhea.[2] Parenti and co-workers recently developed injectable formulations of ramoplanin particularly suitable for intravenous administration.[47] These formulations were well tolerated and are particularly effective in treating severe Gram-positive bacterial infections. Other potential applications include topical use for treatment of acne,[29,37] open wounds,[29] and skin grafts.[48]

MECHANISM OF ACTION

Ramoplanin Alters Bacterial Cell Wall Peptidoglycan Architecture and Integrity

Ramoplanin causes alterations to cell wall peptidoglycan linkages and membrane permeability of Gram-

positive bacteria. Liquid chromatography-mass spectrometry (LC-MS) analyses of the peptidoglycan nucleotide precursor contents of enterococci and staphylococci treated with ramoplanin, tunicamycin, or vancomycin were carried out by van Heijenoort and co-workers.[49] In all cases, a sharp increase in the UDP–*N*-acetylmuramoyl–pentapeptide or –pentadepsipeptide pool was observed. Concomitantly, new peptidoglycan nucleotide peptides of higher molecular masses with hexa- or heptapeptide moieties were identified: UDP–MurNAc–pentapeptide–Asp or pentadepsipeptide–Asp in enterococci, and UDP–MurNAc–pentapeptide–Gly or –Ala and UDP–MurNAc–pentapeptide–Gly–Gly or –Ala–Gly in staphylococci.

Reynolds and Somner observed that ramoplanin disrupts the integrity of the bacterial cell wall.[50] It was found that bacteria treated with high concentrations of ramoplanin released UV-active cellular contents into the culture medium. Electron microscopy studies of the effects of ramoplanin on Gram-positive bacteria cell wall ultrastructure are in progress (D. McCafferty, unpublished results).

Ramoplanin Inhibits the MurG and Transglycosylase Glycosyltransferase Enzymes by a Mechanism that Involves Sequestration of Peptidoglycan Biosynthesis Lipid Intermediates

Ramoplanin acts by inhibiting the late stage assembly of the peptidoglycan monomer and its polymerization into mature peptidoglycan (Figure 2). Reynolds and Somner first determined that ramoplanin inhibits the ability of the MurG glycosyltransferase to convert undecaprenyl–pyrophosphoryl–*N*-acetylmuramyl–pentapeptide (Lipid I) and uridyl–pyrophosphoryl–*N*-acetylglucoseamine (UDP–GlcNAc) into uridyl–diphosphate (UDP) and undecaprenyl–pyrophosphoryl–*N*-acetylmuramyl–(*N*-acetylglucoseamine)–pentapeptide (Lipid II, see Figure 2).[50] Reynolds further astutely postulated that this mechanism of inhibition might involve complexation of Lipid I by ramoplanin since its antimicrobial activity was increased dramatically as levels of the antibiotic approached concentrations equivalent to predicted cellular pool levels of Lipid I. Work by van Heijenoort and colleagues confirmed inhibition of MurG by ramoplanin (50 μM) *in vitro* using recombinant, detergent solublized His_6-tagged enzyme and a synthetic Lipid I analogue.[51,52]

Sahl and co-workers provided the first evidence that ramoplanin interacts with Lipid intermediates.[53] They showed that thin layer chromatographic migration profiles of both Lipid I and Lipid II were altered in the presence of the antibiotic, suggesting that the two form a complex. Since both Lipid I and II were observed to bind ramoplanin, the possibility was raised that the antibiotic might also interfere with transglycosylation via capture of Lipid II. Using citronellyl–Lipid II, a soluble synthetic analogue of Lipid II, Walker and co-workers subsequently confirmed that ramoplanin indeed possessed this second peptidoglycan biosynthesis inhibitory activity by directly showing its inhibition of extracellular transglycosylase activity.[54] Importantly, upon complexation with citronellyl–Lipid II, Walker showed that ramoplanin underwent a ligand-induced aggregation to produce insoluble fibrils, precluding molecular characterization of the inhibitory complex. McCafferty and co-workers subsequently confirmed that complexation and fibril formation was not restricted to Lipid II, since the synthetic Lipid I analogue citronellyl–Lipid I and the related peptidoglycan biosynthesis precursors UDP–MurNAc–L-Ala–γ-D-Glu–*meso*-Dap–D-Ala–D-Ala (also known as UDP–MurNAc–pentapeptide or Park's nucleotide) and UDP–MurNAc–L-Ala–γ-D-Glu–*meso*-Dap (UDP–MurNAc–tripeptide) were found to bind to ramoplanin with high affinity. Like Lipid II, these structurally related compounds formed insoluble fibrils following complexation with ramoplanin (Figure 9).[55]

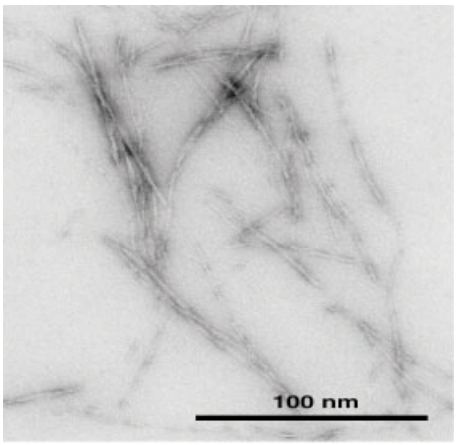

FIGURE 9 Transmission electron micrograph of the fibrils formed from the complexation of ramoplanin A2 with a soluble analogue of Lipid I, citronellyl–Lipid I. Similar fibrils have been observed to form from the complexation of ramoplanin with citronellyl–Lipid II, UDP–MurNAc–pentapeptide (Park's nucleotide), and UDP–MurNAc–tripeptide.

McCafferty and colleagues observed that the addition of 20% DMSO during titrations of ramoplanin with peptidoglycan-derived monomers prevented or considerably reduced fibril formation of the complex. However, significant binding affinity for peptidoglycan intermediates and related analogues was preserved, thus facilitating both the determination of dissociation

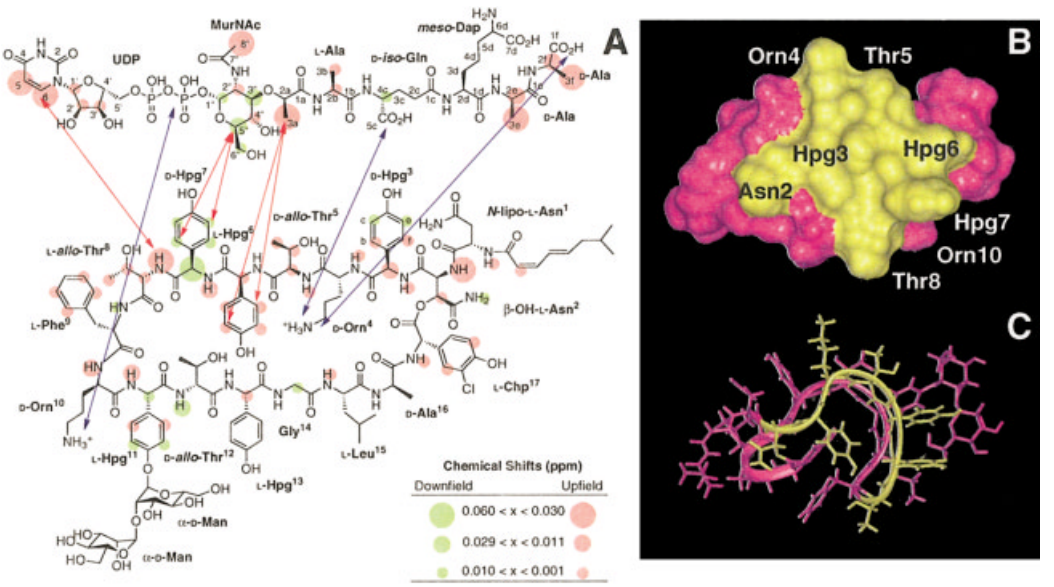

FIGURE 10 (A) NMR localization of the binding interface between ramoplanin A2 and Park's nucleotide (1:1 molar ratio). Protons that exhibit downfield chemical shifts upon binding are colored green; those that shift upfield are depicted in orange. Protons that do not shift upon binding are colorless. Intermolecular NOEs are depicted by red arrows. Possible anchoring electrostatic interactions between ramoplanin Orn^{4},Orn^{10} residues and Park's nucleotide are indicated by blue arrows. NMR experiments further localize the minimum peptidoglycan structure recognized by ramoplanin to the intact pyrophosphate, the muramyl carbohydrate, and the first two amino acids of the pentapeptide. (B) Surface localization of the peptidoglycan monomer/lipid intermediate binding region of ramoplanin. Residues comprising the binding interface identified by NMR that lie on the same face of the antibiotic are colored yellow and mapped onto (C) the three-dimensional NMR structure of ramoplanin obtained in 20% DMSO.

constants for the complex and the identification of the binding interface by NMR methods.[55] NMR analysis in conjunction with chemical dissection of the peptidoglycan monomer revealed that the ramoplanin octapeptide D-Hpg–D-Orn–D-*allo*Thr–Hpg–D-Hpg–*allo*Thr–Phe–D-Orn recognizes MurNAc–Ala–γ-D-Glu pyrophosphate, the minimum component of peptidoglycan capable of high affinity complexation and fibril formation (Figure 10). Ramoplanin therefore recognizes a novel peptidoglycan binding locus different from the *N*-acyl–D-Ala–D-Ala moiety targeted by vancomycin.

McCafferty and co-workers determined that ramoplanin's cup-shaped central two-stranded β-sheet flattens upon complexation with peptidoglycan biosynthesis intermediates.[55] In solution, this conformational change exposes the Phe^{9}–Chp^{17}–Hpg^{3} hydrophobic core to bulk solvent, creating a newly exposed hydrophobic face capable of dimerization and oligomerization with other complexes. This is likely the physical basis of the ligand-induced fibril formation that is observed in aqueous solution in the absence of 20% DMSO. Fibril formation might be precluded in a membrane environment. Although the membrane-bound conformation of ramoplanin has not yet been established, Walker and co-workers recently showed that in deuterated methanol, a solvent chosen to purportedly mimic the dielectric constant of a water–membrane interface, ramoplanin exists as an equilibrium mixture of monomer and homodimer at millimolar (mM) concentrations.[56] In the NMR structure of the homodimer, residues Orn^{10}–Gly^{14} from each monomer form two bent antiparallel β-strands with four hydrogen bonds acting to stabilize the interface, forming a purported peptidoglycan monomer binding pocket flanked by Orn^{4} and Orn^{10} (Figure 11). However, the residues comprising this pocket and the dimer interface are not those identified as making critical contacts with peptidoglycan monomers as assessed by solution NMR and chemical modification studies.[55] In fact, residues that are believed to assist in capture of peptidoglycan monomers lie on the outer solvent-exposed surface of the dimer structure.[55] Since ramoplanin's MIC values are in the 0.03 μg/mL range and no dimer formation is observed in aqueous solution at concentrations up to 5 mM, the

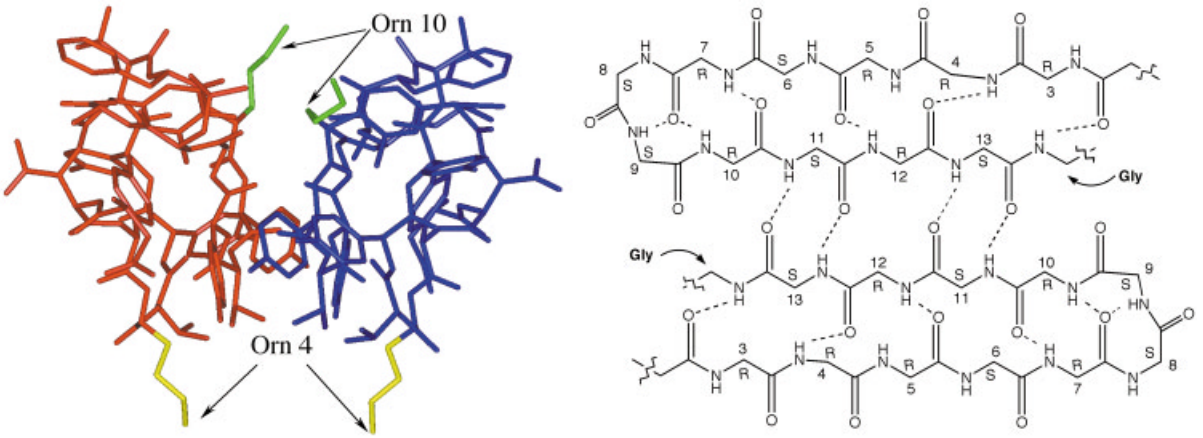

FIGURE 11 Left panel: Three-dimensional structure of the antiparallel ramoplanin A2 dimer that forms at mM concentrations in deuterated methanol as determined by Walker. Right panel: Antiparallel arrangement of the ramoplanin A2 molecules in the homodimer depicting the four intermolecular hydrogen bonds that define the interface.

physiological significance, if any, of methanol-induced dimer formation of the unliganded antibiotic is not clear. However, the conformational changes observed by ramoplanin in solution when complexed to peptidoglycan biosynthesis intermediates[54,55] and concomitant intercomplex aggregation certainly raise the possibility that oligomerization might occur at the level of the membrane, where it would be expected to impart beneficial avidity effects for capture of peptidoglycan monomers or actively polymerizing peptidoglycan chains.

Importantly, no detailed kinetic data is yet available to delineate whether ramoplanin acts to inhibit MurG and/or TGases by substrate depletion (providing a characteristic sigmoidal velocity vs substrate rate profile), or whether the ramoplanin–Lipid intermediate complex is itself a competitive inhibitor of these enzymes. Understanding the true mechanism of ramoplanin is complicated further since the cellular localization of ramoplanin is unknown. As ramoplanin diffuses to the level of the bacterial cell surface, it likely encounters extracellular membrane-associated TGase enzymes, Lipid II, and other actively polymerizing peptidoglycan chains. Although inhibition of TGase activity may be the main basis of ramoplanin's antimicrobial activity, if the antibiotic is capable of translocating across the phospholipid bilayer, if it can capture Lipid I when associated with the outer face of the cell membrane, or if it can interact with MurG/Lipid I when membrane associated, then MurG inhibition could play a significant role in its mechanism of action. Ramoplanin can efficiently anchor to membrane-mimicking unilamellar phospholipid vesicles and micelles (D. McCafferty, unpublished results) suggesting that the antibiotic likely physically interacts with the outer membrane of bacteria. MurG is peripherally associated to the inner cytoplasmic face of the outer membrane,[57] and Lipid I and II are membrane-anchored by a C_{55} undecaprenyl unit that large enough to span a phospholipid bilayer. Due to this large undecaprenyl appendage, one might expect that translocation of Lipid I may be entropically favored. Lastly, it is not yet known if the late-stage peptidoglycan biosynthesis enzymes MraY, MurG, and the TGases are part of a membrane-spanning murein synthase holoenzyme complex that is susceptible to the effects of ramoplanin.[58] Like numerous antibiotics such as vancomycin and nisin, ramoplanin may be evolutionarily optimized to kill bacteria by multiple mechanisms.[59] It is clearly too early to assign a single definitive mechanism of action to ramoplanin.

Structurally Related Antibiotics: The Enduracidins and Janiemycin

A substructure search of the ramoplanin Hpg^3–Orn^{10} peptidoglycan recognition sequence in known peptide antibiotics yielded the enduracidin family of cell wall active lipodepsipeptide antibiotics (Figure 12).[60,61] Produced by *Streptomyces fungicidicus* B5477, enduracidins A (**5**) and B (**6**) are active against Gram-positive bacteria,[62–66] avian myeloblastosis virus reverse transcriptase,[67] hepatitis B virus,[68] and prolyl endopeptidase.[69] Enduracidins have been primarily employed as feed additives to promote livestock growth. The enduracidins contain the sequence *allo-*

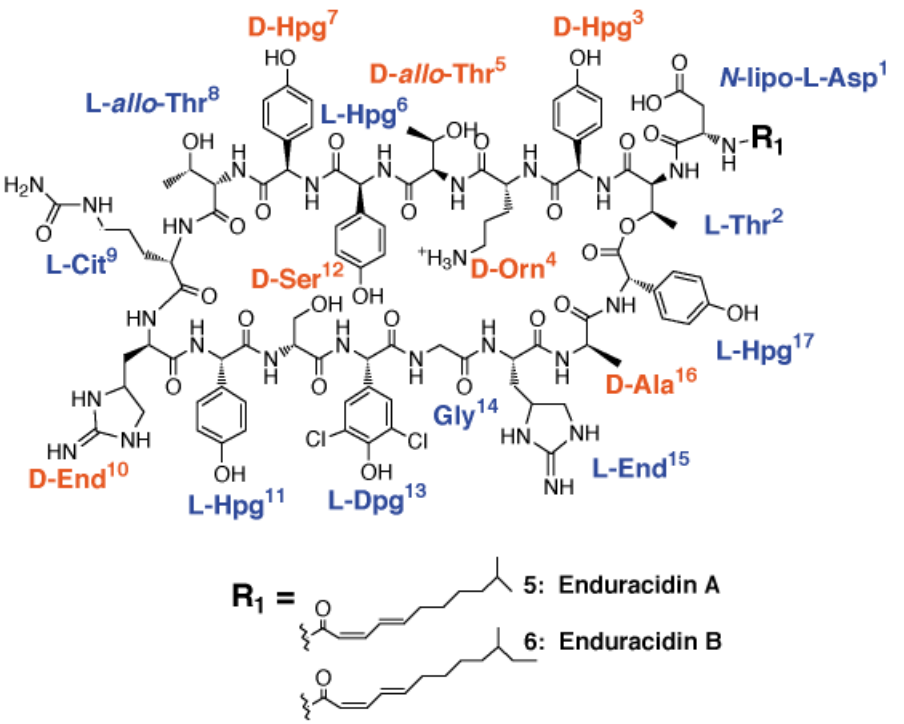

FIGURE 12 Chemical structure of the antibiotics enduracidin A and B. D-Amino acids are depicted in red, L-amino acids are depicted in blue. Nonstandard residues are denoted as follows: Cit, citrulline; Dpg, 3,5-dichloro-4-hydroxyphenylglycine; End, enduracididine.

Thr^{8}-D-Hpg^{7}–Hpg^{6}–D-*allo*-Thr^{5}-D-Orn^{4}–D-Hpg^{3} that exhibits close sequence similarity to ramoplanin's Hpg^{3}–Orn^{10} peptidoglycan recognition sequence (Figure 12). Enduracidin and ramoplanin share a number of additional structural similarities that point to similar mechanisms of action and a common bioactive antibiotic pharmacophore.[61] This was confirmed recently by McCafferty and co-workers, who showed that, like ramoplanin, the enduracidins bind to peptidoglycan lipid intermediates.[61]

Ramoplanin A2 is also related structurally to the peptide antibiotic janiemycin, a cell wall biosynthesis inhibitor produced by *Streptomyces macrosporeus.*[70] Janiemycin shares a similar amino acid composition with enduracidin,[70] although further structural analysis of this peptide has not been reported. Like ramoplanin A2, bacteria treated with janiemycin accumulate lipid intermediates.[71,72] Given the amino acid similarity of janiemycin to the ramoplanins and the enduracidins, it is likely that janiemycin also inhibits TGase and/or MurG activity by a mechanism involving Lipid I and/or II binding.

Ramoplanin is Functionally Related to Lipid II Binding Lantibiotics and Glycopeptides

In addition to the glycopeptides, a growing number of antibiotics have been found to sequester Lipid II as a fundamental part of their mechanism of action.[59] These include two members of the pore-forming type A lantibiotics nisin and epidermin, and the two type B lantibiotic transglycosylase inhibitors mersacidin and actagardine.[73,74] The primary sequences of nisin, epidermin, mersacidin, and actagardine appear in Figure 13. Comparison of ramoplanin with nisin and epidermin[73] indicates no conservation of primary or secondary structure, although these conformationally flexible pore-forming antibiotics are known to bind to Lipid II prior to membrane disruption.[53,75,76] Mutants of nisin with reduced capacity for pore formation still kill bacteria by inhibition of peptidoglycan synthesis via Lipid II sequestration.[76] Mersacidin and actagardine are conformationally constrained globular lantibiotics that inhibit the transglycosylation step of peptidoglycan biosynthesis in a mechanism that involves the formation of a high affinity complex with Lipid II.[77,78] Sahl and co-workers showed that mersacidin targets the MurNAc–GlcNAc disaccharide and pyrophosphate functionalities of Lipid II.[78] The Lipid II subdomain recognized by mersacidin is strikingly similar to the minimal peptidoglycan binding region identified for ramoplanin.[55] Comparison of the solution NMR structures of ramoplanin,[7] mersacidin,[79] and actagardine[80] also reveal a conserved backbone fold (Figure 14).[59,61] Preser-

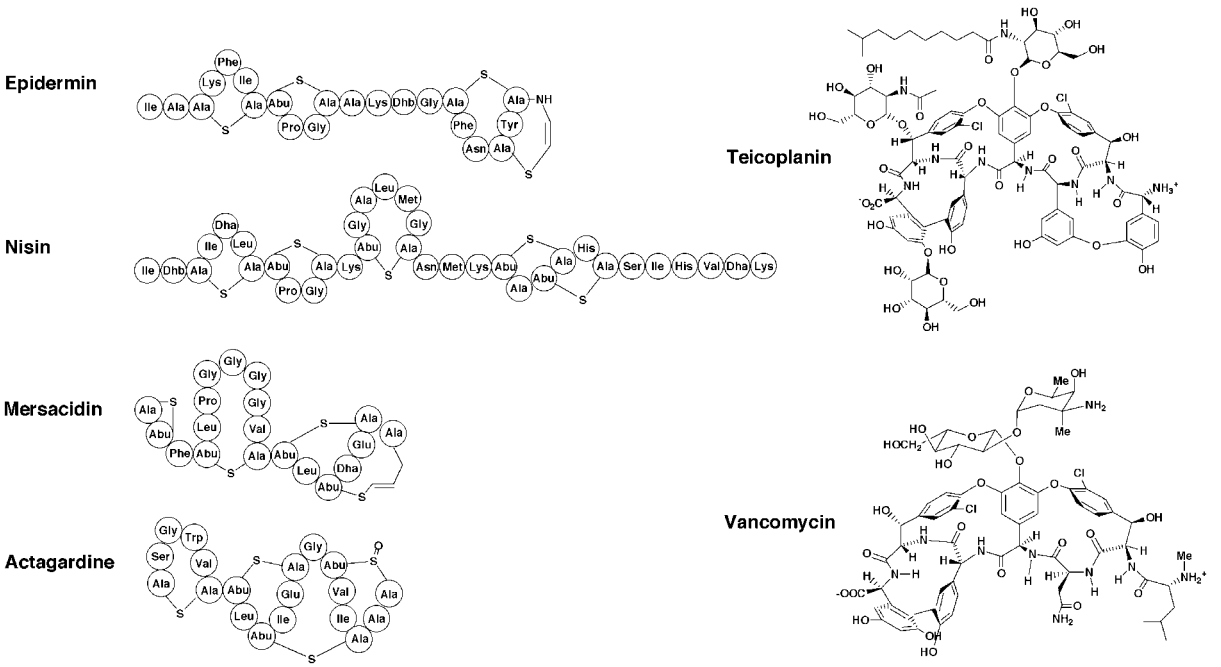

FIGURE 13 Primary sequences of the Lipid intermediate II binding lantibiotics nisin, epidermin, actagardine, and mersacidin, and glycopeptides vancomycin and teicoplanin. Nonstandard residues are denoted as follows: Abu, aminoisobutyric acid; Dha, didehydroalanine; Dhb, didehydrobutyrine.

vation of this overall fold between these Lipid II-binding antibiotics is suggestive of overlapping Lipid II binding sites and a common mechanism of action.[55,59,73,80–82]

Ramoplanin is also functionally related to glycopeptide antibiotics such as vancomycin and teicoplanin (Figure 13). Though these antibiotics bear no sequence or structural similarity to ramoplanin,

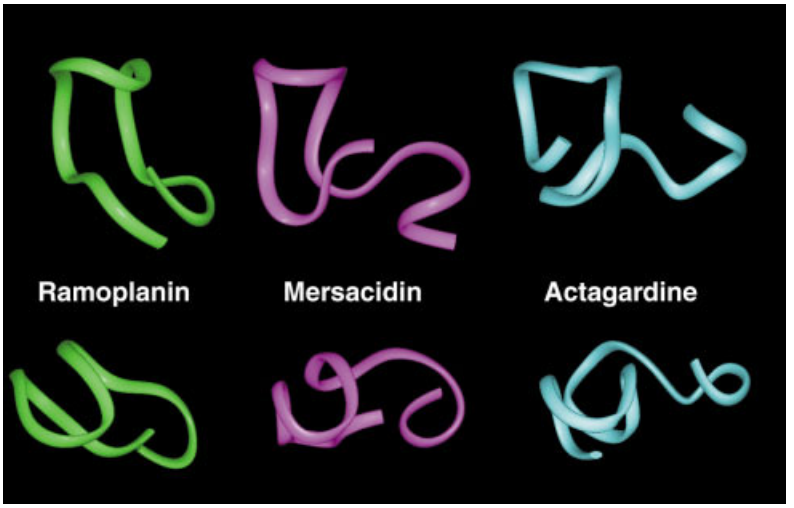

FIGURE 14 Tertiary backbone structures of ramoplanin A2 (green) and two functionally related type B lantibiotics, mersacidin (magenta) and actagardine (blue). Ribbon representations of the tertiary structures were drawn using the program Insight II. Coordinates for ramoplanin (1DSR) and actagardine (1AJ1) NMR structures have been deposited in the Protein Data Bank. NMR coordinates for mersacidin were kindly provided by Dr. Thomas Prasch (Johann Wolfgang Goethe-Universitate, Frankfurt).

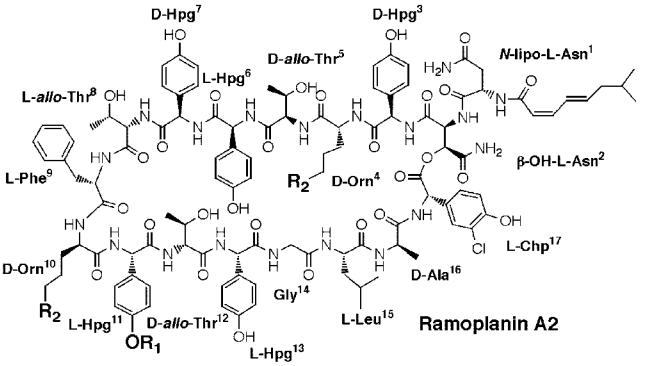

	R_1	R_2	MIC (μg/mL)	K_d (μM) with UDP-MurNAc-pentapeptide	K_d (μM) with UDP-MurNAc-tripeptide
2	α-D-Mannosyl-(1→2)-α-D-mannose	NH_3^+	0.03	180 ± 20	2,380 ± 440
7	H	NH_3^+	0.03	330 ± 50	1,300 ± 230
8	α-D-Mannosyl-(1→2)-α-D-mannose	$HNC(NH)NH_3^+$	0.25	170 ± 30	no interaction
9	α-D-Mannosyl-(1→2)-α-D-mannose	$HN^+(CH_2)_2CH(CH_3)_2$	4.0	130 ± 20	1,280 ± 140
10	α-D-Mannosyl-(1→2)-α-D-mannose	NHAc	16.0	1,340 ± 320	no interaction
11	α-D-Mannosyl-(1→2)-α-D-mannose	NH_3^+ (Lactone hydrolyzed)	64.0	no interaction	no interaction

FIGURE 15 MIC values of semisynthetic derivatives of ramoplanin A2 and dissociation constants for peptidoglycan intermediate binding.

both are transglycosylase inhibitors that sequester Lipid II during the normal course of their mechanism of action. Whereas glycopeptides bind to the terminal *N*-acyl–D-Ala–D-Ala moiety of Lipid II, ramoplanin targets the MurNAc–(GlcNAc)–Ala–γ-D-Glu pyrophosphate region of Lipid II. Vancomycin resistance is conferred by replacement of the Lipid II terminal D-Ala–D-Ala dipeptide with a D-Ala–D-lactate depsipeptide. The resulting Lipid II depsipeptide functions equivalently as the wild-type substrate for transpeptidation and transglycosylation, yet this oxygen for nitrogen mutation reduces its binding to the antibiotic by 1000-fold.[83,84] The potent activity of ramoplanin against vancomycin-resistant bacterial strains may be explained in part by its ability to target nonoverlapping sites of Lipid intermediate II.

SYNTHETIC STUDIES OF RAMOPLANIN AND RELATED ANALOGUES

Semisynthetic Modifications of Ramoplanin and Ramoplanose

Ramoplanin has been semisynthetically modified for the purposes of improving its antimicrobial activity and for analysis of the structural basis for its mechanism of action. Ciabatti and co-workers prepared derivatives of ramoplanins A1–A3 in which the double bonds of the native *N*-terminal acyl chain were reduced by catalytic hydrogenation over platinum oxide.[85,86] The resulting compounds, intended for use as topical antibiotics for treatment of open wounds, exhibited excellent activity against a variety of Gram-positive bacterial strains.

Aglycons of ramoplanins A1–A3, prepared by Ciabatti and colleagues using trimethylsilyl iodide in dimethylformamide (DMF), exhibited equipotent or slightly better activity than the parent compounds against an array of *S. epidermis, S. aureus,* and *P. acne* strains, suggesting that glycosylation is not essential for antimicrobial activity.[87,88] McCafferty and co-workers determined that glycosylation of ramoplanin A2 only has a slight influence on the energetics of peptidoglycan lipid intermediate monomer binding (Figure 15).[61] Like ramoplanin A2, the aglycon (compound **7,** Figure 15) also formed fibrils with peptidoglycan biosynthesis intermediates and related analogues.[61] However, removal of the disaccharide also increased conformational flexibility and susceptibility of the aglycon to acid hydrolysis. Since the aglycon contains the full complement of wild-type ramoplanin's antimicrobial activity, removal of the mannosyl disaccharide from ramoplanin A2 leads to a bioactive pharmacophore with significantly reduced chemical complexity.

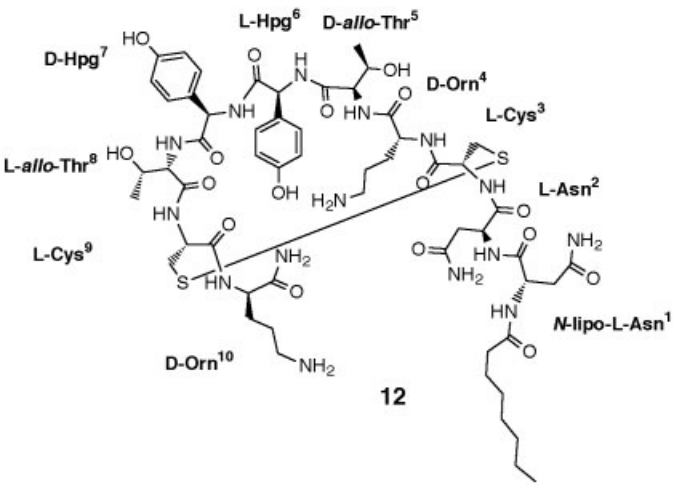

FIGURE 16 Covalent structure of a disulfide-linked lipopeptide with peptidoglycan binding activity based on the Hpg^3–Orn^{10} peptidoglycan binding motif of ramoplanin A2.

To examine the involvement of ramoplanin's two ornithine residues (Orn^4 and Orn^{10}) within the Hpg^3–Orn^{10} peptidoglycan recognition sequence in peptidoglycan monomer recognition and fibril formation, McCafferty and co-workers prepared semisynthetic analogues in which the Orn residues were side chain modified by guanidylation (**8**), reductive amination (**9**), and acetylation (**10**) (Figure 15).[61] It was found that increasing dissociation constants of derivatives binding to peptidoglycan biosynthesis intermediates were paralleled by increasing MIC values (Figure 15). Loss of cationic charge by acetylation severely reduced antimicrobial activity and eliminated binding to peptidoglycan monomers and related analogues, in turn abolishing fibril formation. Preservation of cationic charge by guanidylation and reductive amination of these sites resulted in only small to modest alterations to antimicrobial

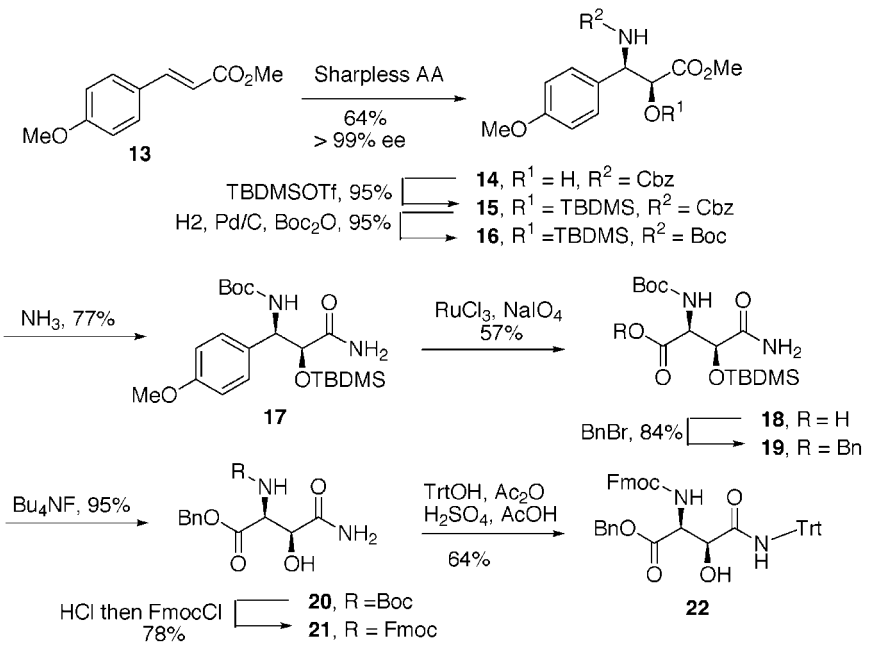

FIGURE 17 Boger's synthesis of a protected form of *threo*-β-hydroxy-L-asparagine for use in the total synthesis of ramoplanin A2.

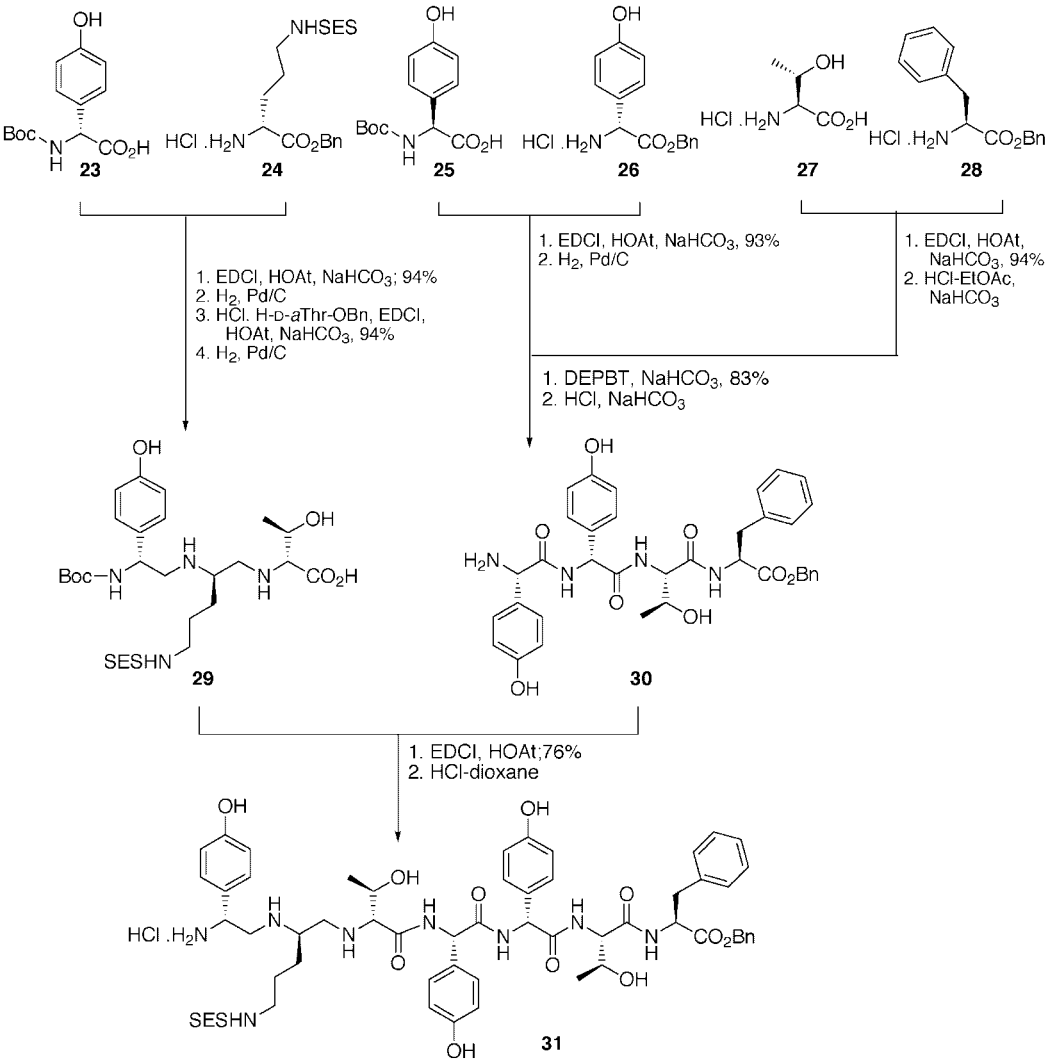

FIGURE 18 Synthesis of ramoplanin A2 and ramoplanose aglycon. Part I: Assembly of the protected D-Hpg–D-Orn–D-*allo*Thr–Hpg–D-Hpg–*allo*Thr–Phe heptapeptide subunit.

activity, peptidoglycan monomer binding, and fibril formation propensity as compared to ramoplanin A2. Orn^4 and Orn^{10} likely interact with the pyrophosphate and terminal carboxylate of Lipid I/II. The strong correlation between the presence of cationic charges on the Orn^4,Orn^{10} side-chain amino groups and the affinity of the antibiotic toward peptidoglycan precursors suggests that these residues anchor the peptidoglycan ligand in the proper orientation for binding using electrostatic or hydrogen-bonding interactions.[61] Preservation of charge on these residues is also essential for antimicrobial activity, with the general order of activity of 1° amine > guanidine > 2° amine for those analogues tested.

Williams and co-workers previously demonstrated that the hydrolyzed linear form of the closely related antibiotic ramoplanose maintained significant native-like β-sheet structure in D_2O after hydrolysis[89]; however, the solubility of this compound was markedly reduced. Similarly, McCafferty and co-workers found that linearized ramoplanin A2 (**11,** Figure 15) also was significantly less soluble than the parent lactone and the antimicrobial activity of this compound was decreased >2000-fold as compared to ramoplanin A2.[61] Linearized ramoplanin A2 did not bind peptidoglycan biosynthesis lipid intermediates or related analogues, suggesting that high affinity capture of these compounds requires presentation of

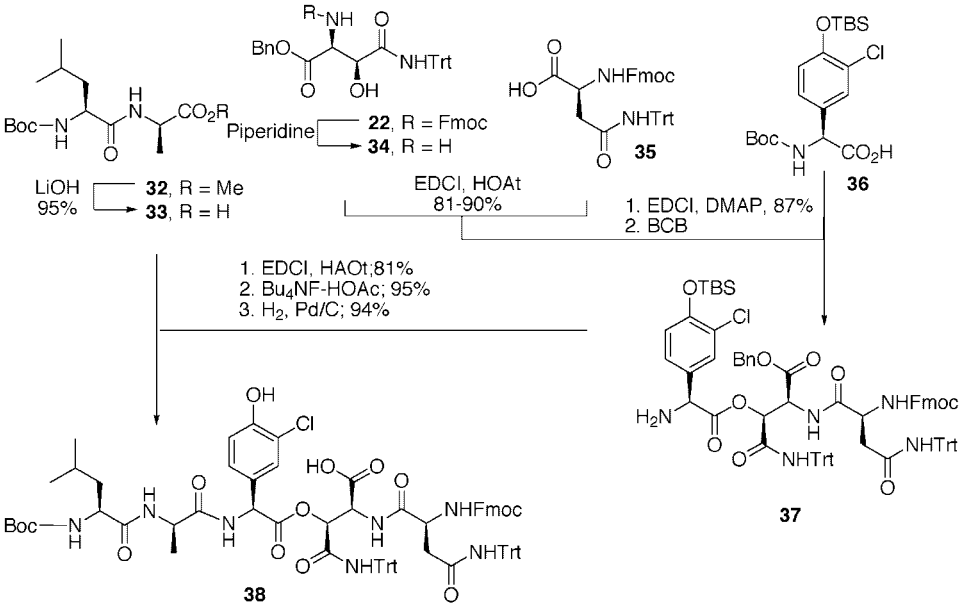

FIGURE 19 Synthesis of ramoplanin A2 and ramoplanose aglycon. Part II: Assembly of the protected Leu–D-Ala–Chp–L-*threo*-β-OH–Asn–Asn subunit.

residues along the Hpg[3]–Orn[10] sequence in a specific three-dimensional conformation (Figure 15). Presentation in its bioactive conformation is facilitated by the constraining Asn[2]–Chp[17] lactone. Evidence in support of a specific bioactive conformation for the Hpg[3]–Orn[10] sequence was recently

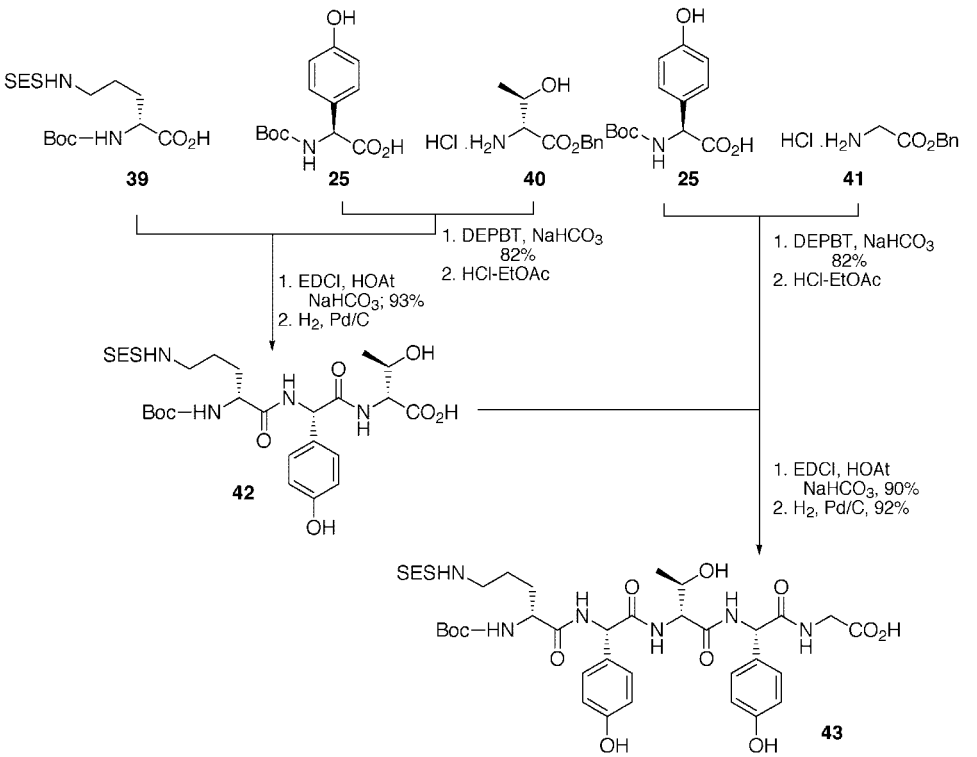

FIGURE 20 Synthesis of ramoplanin A2 and ramoplanose aglycon. Part III: Assembly of the protected D–Orn–Hpg–D-*allo*Thr–Hpg–Gly pentapeptide subunit.

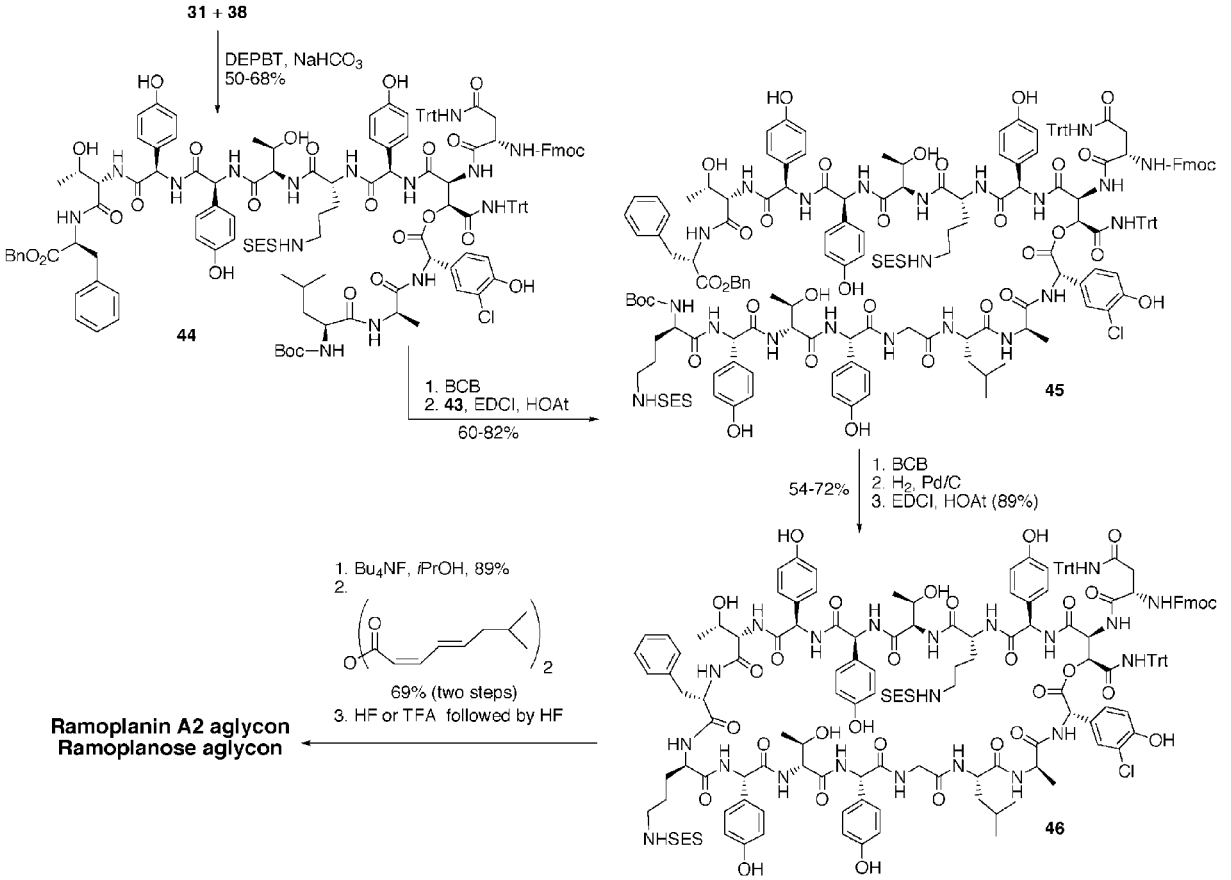

FIGURE 21 Synthesis of ramoplanin A2 and ramoplanose aglycon. Part IV: Assembly of the full-length linear 17-residue depsipeptide, Orn^{10}–Phe^{9} macrocyclization, and end-game deprotection.

obtained since a synthetic cyclic peptide derived from the ramoplanin peptidoglycan recognition sequence, N^{α}-octanoyl–Asn–Asn–*cyclo*[Cys–D-Orn–Phe–*allo*-Thr–D-Hpg–D-*allo*-Thr–Hpg–Cys]–D-Orn–NH_2 (**12**) was shown to bind the peptidoglycan biosynthesis intermediate Park's nucleotide as the conformationally constrained disulfide, but not as the linear free dithiol (Figure 16).[61]

Total Synthesis of the Aglycon of Ramoplanin A2 and Ramoplanose

Boger and co-workers recently reported an elegant solution-phase total synthesis of the aglycon of ramoplanin A2 and ramoplanose (**7,** Figure 15).[90,91] Their strategy was to construct three key protected peptide subunits that were sequentially coupled to form a 17-residue linear protected peptide. This intermediate was subsequently cyclized between Phe^{9} and Orn^{10} to form the 49-membered macrocycle (Figure 1). This macrocyclization site was chosen to take advantage of the beneficial effects of β-sheet preorganization as well as previous reports of efficient peptide macrolactamization at a D-amino acid terminus.[92]

The preparation of the nonstandard amino acid L-*threo*-β-hydroxyasparagine (L-*threo*-β-OH–Asn) was required as a key subunit. Since no enantioselective synthesis of *threo*-β-OH–Asn was known, Boger's group developed a nine-step asymmetric synthesis of L-*threo*-N^{α}-Fmoc–β-OH–Asn(Trt)–OBn (**22**), a protected form of the amino acid suitable for solution-phase assembly of ramoplanin (Figure 17). In Boger's approach, Sharpless aminohydroxylation of cinnamate **13** established the *threo* stereochemistry of the amino and hydroxyl groups. Following functional group transformations to produce compound **17,** the α-carboxylate was liberated from the 4-methoxyphenyl masking group by RuO_4 oxidation. Subsequent functional group transformation and introduction of 9-fluorenylmethoxycarbonyl (Fmoc) and trityl (Trt) protecting groups produced the L-*threo*-β-OH–Asn module **22.**

The first stage of assembly of the protected modular peptides is depicted in Figure 18. Protected amino acids **23–28** were coupled together using either standard carbodiimide activation or 3-(diethoxyphosphoryloxy)-1,2,3-benzotriazin-4(3*H*)-one (DEBPT)[93] (to prevent racemization of Hpg and reduce β-elimination of α-Thr residues) to form tripeptide **29** and tetrapeptide **30.** These intermediates were joined to afford the D-Hpg–D-Orn–D-*a*Thr–Hpg–D-Hpg–*a*Thr–Phe heptapeptide subunit **31.** It is of note that neither Hpg nor *allo*-Thr residues were side chain protected during assembly of the main-chain amide bonds, owing to the lack of reactivity of these residues and the judicious choice of activation reagents. β-Elimination was also suppressed by similar critical evaluation of the experimental conditions employed.

The second key subunit, pentadepsipeptide **38,** was prepared from four protected component pieces: L-*threo*-β-OH–Asn module **22,** Leu–D-Ala dipeptide **32,** and Asn derivative **35** and Chp analogue **36** (Figure 19). Compound **22** was deprotected to afford compound **34,** efficiently coupled to Chp derivative **36** using 1-ethyl-3(3′-dimethylaminopropyl)carbodiimide hydrochloride (EDCI) with the acylation catalyst 4-(*N*,*N*-dimethylamino)pyridine (DMAP), and then deprotected with *B*-bromocatecholborane (for selective Boc group removal) to provide depsipeptide **37.** Dipeptide **32** was deprotected, coupled with **37,** and deprotected to afford the Leu–D-Ala–Chp–L-*threo*-β-OH–Asn–Asn subunit **38.**

The third pentapeptide key subunit **43** was assembled from precursors **25** and **39–41** (Figure 20). Hpg derivative **25** and D-*allo*Thr derivative **40** were efficiently coupled using DEPBT without deleterious racemization. Boc removal followed by acylation with **39** generated tripeptide **42.** Compound **25** was coupled with **41** using DEPBT, deprotected, and joined with **42** to provide the D-Orn–Hpg–D-*allo*Thr–Hpg–Gly pentapeptide (**43**) in excellent yield.

Assembly of the key fragments proved to be the most challenging portion of the synthesis. As depicted in Figure 21, fragments **31** and **38** were coupled using DEPBT to yield depsipeptide **44.** Boc group removal and carbodiimide-mediated coupling with subunit **43** yielded the entire linear 17-residue depsipeptide **45;** at this point in the synthesis all peptide backbone bonds were intact with the exception of the amide bond between Orn^{10} and Phe^{9}. Following deprotection, the Orn^{10}–Phe^{9} macrolactam was efficiently produced (87%) using EDCI/HOAt (1-hydroxy-7-azabenzotriazole) to yield depsipeptide **46.** Selective removal of the *N*-terminal Asn Fmoc protecting group followed by acylation of that site with 7-methyloctadi-2,4-enoic acid (prepared from 5-methyl-hex-2-enal using the Horner–Wadsworth–Emmons methods) and global deprotection with HF yielded the ramoplanose and ramoplanin A2 aglycon (**7,** Figure 15).

CONCLUSIONS

Ramoplanin is a promising clinical candidate for treatment of VRE and MRSA infections. Presently the antibiotic is in Phase III trials for oral treatment of enterococcal infections. Ramoplanin is significantly more potent than vancomycin for treatment of Gram-positive bacterial infections, although the lack of absorption of the antibiotic has limited its development as a general replacement for vancomycin to date. Detailed mechanism of action and structure/activity studies have shed light on the molecular basis for its bacterial killing mechanism. However, many critical issues remain unresolved, such as the unknown capacity of the antibiotic to translocate into the bacterial cell, the significance of the phenomenon of Lipid intermediate capture and intercomplex aggregation, and the identity of the ramoplanin bioactive pharmacophore. Regardless, ramoplanin and its derivatives will find increasing use in dissecting the poorly understood late-stage steps of peptidoglycan biosynthesis and murein sacculus turnover. The development of a new total synthesis of the aglycon now makes possible the development of ramoplanin-derived peptide or peptidomimetic antibiotics with improved activity, absorption, and physiochemical properties for use against VRE, MRSA, and related bacterial pathogens.

We gratefully acknowledge members of the McCafferty laboratory for critical evaluation of the manuscript. This work was generously supported by American Cancer Society grant RPG-99-31-02-CCE, National Institutes of Health grant AI46611, and a grant from the McCabe Foundation. Brenda Frankel is the recipient of a 2001 National Science Foundation Predoctoral fellowship.

REFERENCES

1. Cavalleri, B.; Pagani, H.; Volpe, G.; Selva, E.; Parenti, F. J Antibiot 1984, 37, 309–317.
2. Parenti, F.; Ciabatti, R.; Cavalleri, B.; Kettenring, J. Drugs Exp Clin Res 1990, 16, 451–455.
3. Gastaldo, L.; Ciabatti, R.; Assi, F.; Restelli, E.; Kettenring, J. K.; Zerilli, L. F.; Romano, G.; Denaro, M.; Cavalleri, B. J Ind Microbiol 1992, 11, 13–18.
4. Ciabatti, R.; Kettenring, J. K.; Winters, G.; Tuan, G.; Zerilli, L.; Cavalleri, B. J Antibiot 1989, 42, 254–267.
5. Kettenring, J. K.; Ciabatti, R.; Winters, G.; Tamborini, G.; Cavalleri, B. J Antibiot 1989, 42, 268–275.

6. Skelton, N. J.; Harding, M. M.; Mortishire-Smith, R. J.; Rahman, S. K.; Williams, D. H.; Rance, M. J.; Ruddock, J. C. J Am Chem Soc 1991, 113, 7522–7530.
7. Kurz, M.; Guba, W. Biochemistry 1996, 35, 12570–12575.
8. Stachelhaus, T.; Mootz, H. D.; Marahiel, M. A. Chem Biol 1999, 6, 493–505.
9. Challis, G. L.; Ravel, J.; Townsend, C. A. Chem Biol 2000, 7, 211–224.
10. Quadri, L. E. N.; Sello, J.; Keating, T. A.; Weinreb, P. H.; Walsh, C. T. Chem Biol 1998, 5, 631–645.
11. Farnet, C. M.; Zazopoulos, E.; Staffa, A. In PCT Int Appl (Ecopia Biosciences Inc., Can.).: Wo 0231155, 2002; 212 pp.
12. van Wageningen, A. M.; Kirkpatrick, P. N.; Williams, D. H.; Harris, B. R.; Kershaw, J. K.; Lennard, N. J.; Jones, M.; Jones, S. J.; Solenberg, P. J Chem Biol 1998, 5, 155–162.
13. Hubbard, B. K.; Thomas, M. G.; Walsh, C. T. Chem Biol 2000, 7, 931–942.
14. Chiu, H. T.; Hubbard, B. K.; Shah, A. N.; Eide, J.; Fredenburg, R. A.; Walsh, C. T.; Khosla, C. Proc Natl Acad Sci USA 2001, 98, 8548–8553.
15. Espersen, F. Curr Opin Anti-Infect Invest Drugs 1999, 1, 78–86.
16. Jones, R. N.; Barry, A. L. Diag Microbiol Infect Dis 1989, 12, 279–282.
17. Neu, H. C.; Neu, N. M. Chemotherapy (Basel) 1986, 32, 453–457.
18. Shonekan, D.; Mildvan, D.; Handwerger, S. Antimicrob Agents Chemother 1992, 36, 1570–1572.
19. Cooper, B.; Robinson, A.; Freeman, C.; Quintiliani, R.; Mazens-Sullivan, M. ICAAC 1993, 33.
20. Rolston, K. V.; Dholakia, N.; Ho, D. H.; LeBlanc, B.; Dvorak, T.; Streeter, H. J Antimicrob Chemother 1996, 38, 265–269.
21. Venditti, M.; Tarasi, A.; Gelfusa, V.; Nicastri, E.; Penni, A.; Martino, P. Antimicrob Agents Chemother 1993, 37, 1190–1192.
22. Collins, L. A.; Eliopoulos, G. M.; Wennersten, C. B.; Ferraro, M. J.; Moellering, R. C., Jr. Antimicrob Agents Chemother 1993, 37, 1364–1366.
23. Johnson, C. C.; Taylor, S.; Pitsakis, P.; May, P.; Levison, M. E. Antimicrob Agents Chemother 1992, 36, 2342–2345.
24. O'Hare, M. D.; Ghosh, G.; Felmingham, D.; Gruneberg, R. N. J Antimicrob Chemother 1990, 25, 217–220.
25. van der Auwera, P.; Couvreur, M. L.; Grenier, P.; Vandermies, A.; Kaufman, L.; Derde, M. P.; Mertens, R.; Struelens, M. ICAAC 1993, 33, 296.
26. Woodford, N.; Patel, S.; Johnson, A. P.; Farrelly, H.; Cookson, B. ICAAC 1993, 33, 309.
27. Lawrence, T.; Rotstein, C.; Beam, T. R.; Gorzynski, E. A.; Amsterdam, D. Antimicrob Agents Chemother 1993, 37, 896–900.
28. Rodrigues, J. N.; Amaral, J. L. G.; Leme, I. L.; Pignatari, A.; Wey, S.; Hollis, R.; Pfaller, M. A.; Jones, R. N. Diagn Microbiol Infect Dis 1993, 16, 9–16.
29. O'Hare, M. D.; Felmingham, D.; Gruneberg, R. N. Drugs Exp Clin Res 1988, 14, 617–619.
30. Maple, P. A. C.; Hamilton-Miller, J. M. T.; Brumfitt, W. J Antimicrob Chemother 1989, 23, 517–525.
31. Maple, P. A.; Hamilton-Miller, J. M.; Brumfitt, W. Lancet 1989, 1, 537–540.
32. Bartoloni, A.; Colao, M. G.; Orsi, A.; Dei, R.; Giganti, E.; Parenti, F. J Antimicrob Chemother 1990, 26, 627–633.
33. Neal, T. J.; O'Donoghue, M. A. T.; Ridgway, E. J.; Allen, K. D. J Antimicrob Chemother 1992, 30, 39–46.
34. Pallanza, R.; Scotti, R.; Beretta, G.; Cavalleri, B.; Arioli, V. Antimicrob Agents Chemother 1984, 26, 462–465.
35. Dworczynski, A.; Martirosian, G.; Meisel-Mikolajczyk, F. Med Dosw Mikrobiol 1993, 45, 483–486.
36. Biavasco, F.; Manso, E.; Varaldo, P. E. Antimicrob Agents Chemother 1991, 35, 195–197.
37. O'Hare, M. D.; Ghosh, G.; Felmingham, D.; Grueneberg, R. N. J Antimicrob Chemother 1990, 25, 217–220.
38. Francis, J.; Webster, H.; Newsom, S. W. B. Drugs Exp Clin Res 1990, 16, 457–460.
39. Ristow, T. A.; Noskin, G. A.; Warren, J. R.; Peterson, L. R. Microb Drug Resist 1995, 1, 335–339.
40. Mobarakai, N.; Quale, J. M.; Landman, D. Antimicrob Agents Chemother 1994, 38, 385–387.
41. Scotti, R.; Dulworth, J. K.; Kenny, M. T.; Goldstein, B. P. Diagn Microbiol Infect Dis 1993, 17, 209–211.
42. Romeo, B.; Lealil, G. M.; Borgonovi, M.; Cavenaghi, L.; Hinze, C.; Kaschube, M.; Seppala, A.; Gardner, S. Microbial Ecol Health Disease 1992, 2, 6.
43. Romeo, B.; Kaschube, M.; Cavenaghi, L.; Borgonovi, M.; Jaulhac, B.; Monteil, H.; Gardner, S.; Seppala, A. ICAAC 1993, 33, 200.
44. Whitman, M. S.; Pitsakis, P. G.; DeJesus, E.; Osborne, A. J.; Levison, M. E.; Johnson, C. C. Antimicrob Agents Chemother 1996, 40, 1526–1530.
45. Wong, M. T.; Kauffman, C. A.; Standiford, H. C.; Linden, P.; Fort, G.; Fuchs, H. J.; Porter, S. B.; Wenzel, R. P. Clin Infect Dis 2001, 33, 1476–1482.
46. Baden, L. R.; Critchley, I. A.; Sahm, D. F.; So, W.; Gedde, M.; Porter, S.; Moellering, R. C., Jr.; Eliopoulos, G. J Clin Microbiol 2002, 40, 1160–1163.
47. Parenti, F.; Candiani, G.; Ciabatti, R.; Cavaleri, M. In Eur Pat Appl (Biosearch Italia SPA, Italy): Ep 976394, 2000; 17 pp.
48. Holder, I. A.; Boyce, S. T. J Antimicrob Chemother 1996, 38, 457–463.
49. Billot-Klein, D.; Shlaes, D.; Bryant, D.; Bell, D.; Legrand, R.; Gutmann, L.; van Heijenoort, J. J Bacteriol 1997, 179, 4684–4688.
50. Somner, E. A.; Reynolds, P. E. Antimicrob Agents Chemother 1990, 34, 413–419.
51. Auger, G.; Crouvoisier, M.; Caroff, M.; van Heijenoort, J.; Blanot, D. Lett Peptide Sci 1997, 4, 371–376.
52. Crouvoisier, M.; Mengin-Lecreulx, D.; van Heijenoort, J. FEBS Lett 1999, 449, 289–292.

53. Brotz, H.; Josten, M.; Wiedemann, I.; Schneider, U.; Gotz, F.; Bierbaum, G.; Sahl, H.-G. Mol Microbiol 1998, 30, 317–327.
54. Lo, M. C.; Men, H.; Branstrom, A.; Helm, J.; Yao, N.; Goldman, R.; Walker, S. J Am Chem Soc 2000, 122, 3540–3541.
55. Cudic, P.; Kranz, J.; Behenna, D. C.; Kruger, R. G.; Tadesse, H.; Wand, A. J.; Veklich, Y. I.; Weisel, J. W.; McCafferty, D. G. Proc Natl Acad Sci USA 2002, 99, 7384–7389.
56. Lo, M.-C.; Helm, J. S.; Sarngadharan, G.; Pelczer, I.; Walker, S. J Am Chem Soc 2001, 123, 8640–8641.
57. Mengin-Lecreulx, D.; Texier, L.; Rousseau, M.; van Heijenoort, J. J Bacteriol 1991, 173, 4625–4636.
58. Holtje, J. V. Microbiol Mol Biol Rev 1998, 62, 181–203.
59. McCafferty, D. G.; Cudic, P.; Yu, M. K.; Behenna, D. C.; Kruger, R. Curr Opin Chem Biol 1999, 3, 672–680.
60. Higashide, E.; Hatano, K.; Shibata, M.; Nakazawa, K. J Antibiot 1968, 21, 126–137.
61. Cudic, P.; Behenna, D. C.; Kranz, J.; Kruger, R. G.; Wand, A. J.; Veklich, Y. I.; Weisel, J. W.; McCafferty, D. G. Chem Biol 2002, 9, 897–906.
62. Kawakami, M.; Nagai, Y.; Fuji, T.; Mitsuhashi, S. J Antibiot 1971, 24, 583–586.
63. Matsumoto, K.; Miwa, H.; Adachi, M.; Nakazawa, S. Chemotherapy 1973, 21, 531–535.
64. Lugtenberg, E. J. J.; Van Schijndel-Van Dam, A.; Van Bellegem, T. H. M. J Bacteriol 1971, 108, 20–29.
65. Yourassowsky, E.; Monsieur, R. Chemotherapy 1972, 17, 182–187.
66. Tsuchiya, K.; Kondo, M.; Oishi, T.; Yamazaki, T. J Antibiot 1968, 21, 147–153.
67. Inouye, Y.; Take, Y.; Nakamura, S.; Nakashima, H.; Yamamoto, N.; Kawaguchi, H. J Antibiot 1987, 40, 100–104.
68. Wu, T.; Huang, H.; Zhou, P. Zhongguo Bingduxue 1998, 13, 45–49.
69. Kimura, K. I.; Kanou, F.; Yamashita, Y.; Yoshimoto, T.; Yoshihama, M. Biosci Biotechnol Biochem 1997, 61, 1754–1756.
70. Meyers, E.; Weisenborn, F. L.; Pansy, F. E.; Slusarchyk, D. S.; Von Saltza, M. H.; Rathnum, M. L.; Parker, W. L. J Antibiot 1970, 23, 502–507.
71. Linnett, P. E.; Strominger, J. L. Antimicrob Agents Chemother 1973, 4, 231–236.
72. Brown, W. E.; Seinerova, V.; Chan, W. M.; Laskin, A. I.; Linnett, P.; Strominger, J. L. Ann NY Acad Sci 1974, 235, 399–405.
73. Bierbaum, G. Chemother J 1999, 8, 204–209.
74. Sahl, H.-G.; Bierbaum, G. Ann Rev Microbiol 1998, 52, 41–79.
75. Breukink, E.; Wiedemann, I.; Van Kraaij, C.; Kuipers, O. P.; Sahl, H.-G.; De Kruijff, B. Science 1999, 286, 2361–2364.
76. Wiedemann, I.; Breukink, E.; Van Kraaij, C.; Kuipers, O. P.; Bierbaum, G.; De Kruijff, B.; Sahl, H.-G. J Biol Chem 2001, 276, 1772–1779.
77. Brotz, H.; Bierbaum, G.; Reynolds, P. E.; Sahl, H.-G. Eur J Biochem 1997, 246, 193–199.
78. Brotz, H.; Bierbaum, G.; Leopold, K.; Reynolds, P. E.; Sahl, H.-G. Antimicrob Agents Chemother 1998, 42, 154–160.
79. Prasch, T.; Nauman, T.; Markert, R. L.; Sattler, M.; Schubert, M.; Schaal, S.; Bauch, M.; Kogler, H.; Greisinger, C. Eur J Biochem 1997, 244, 501–512.
80. Zimmermann, N.; Jung, G. Eur J Biochem 1997, 246, 809–819.
81. Bierbaum, G.; Brotz, H.; Sahl, H.-G. BIOspektrum 1997, 2, 51–55.
82. Guder, A.; Wiedemann, I.; Sahl, H.-G. Biopolymers 2000, 55, 62–73.
83. Walsh, C. T.; Fisher, S. L.; Park, I.-S.; Prahalad, M.; Wu, Z. Chem Biol 1996, 3, 21–28.
84. Williams, D. H. Nat Prod Rep 1996, 469–477.
85. Ciabatti, R.; Cavalleri, B. In Eur Pat Appl (Gruppo Lepetit SPA, Italy): Ep 321696, 1989; 20 pp.
86. Ciabatti, R.; Cavalleri, B. In Gruppo Lepetit, SPA, Italy: US 5,108,988, 1992.
87. Ciabatti, R.; Cavalleri, B. In Eur Pat Appl (Gruppo Lepetit SPA, Italy): Ep. 337203, 1989; 21 pp.
88. Ciabatti, R.; Cavalleri, B. In US Pat Appl (Gruppo Lepetit, SPA, Italy): US 5,491,128, 1996.
89. Maplestone, R. A.; Cox, J. P. L.; Williams, D. H. FEBS Lett 1993, 326, 95–100.
90. Boger, D. L. Med Res Rev 2001, 21, 356–381.
91. Jiang, W.; Wanner, J.; Lee, R. J.; Bounaud, P.-Y.; Boger, D. L. J Am Chem Soc 2002, 124, 5288–5290.
92. Brady, S. F.; Varga, S. L.; Freidinger, R. M.; Schwenk, D. A.; Mendlowski, M.; Holly, F. W.; Veber, D. F. J Org Chem 1979, 44, 3101–3105.
93. Li, H.; Jiang, X.; Ye, Y.-H.; Fan, C.; Romoff, T.; Goodman, M. Org Lett 1999, 1, 91–93.